Palaeogeography, Palaeoclimatology, Palaeoecology 639 (2024) 112055

Contents lists available at ScienceDirect

Palaeogeography, Palaeoclimatology, Palaeoecology

journal homepage: www.elsevier.com/locate/palaeo

Coupling palaeobiology and geochemistry from the Holocene of the southern Adriatic Sea (Gulf of Manfredonia, Italy): Shelf facies patterns and eutrophication trends

Veronica Rossi [a,*], Irene Sammartino [b], Claudio Pellegrini [b], Giulia Barbieri [a], Chiara Teodoro [a], Fabio Trincardi [c], Alessandro Amorosi [a]

[a] Department of Biological, Geological and Environmental Sciences (BiGeA), University of Bologna, Piazza di Porta San Donato 1, 40126 Bologna, Italy
[b] National Research Council (CNR), Institute of Marine Science (ISMAR), Via Gobetti 101, 40129 Bologna, Italy
[c] Consiglio Nazionale delle Ricerche, Piazzale Aldo Moro 7, 00185 Roma, Italy

ARTICLE INFO

Editor: M Elliot

Keywords:
Apulia
Benthic foraminifers
Ostracods
Prodelta
Po River
Gargano Promontory

ABSTRACT

The combined use of the meiofauna (benthic foraminifers and ostracods) and geochemical data from three cores, recovered in distinct bathymetric sectors of the southern Adriatic shelf (Apulia, SE Italy), provides new insights on the relationships between shallow-marine environments, sediment fluxes and eutrophication trends over the last ~7000 years. The stratigraphic distribution of meiofauna assemblages allows distinguishing a variety of facies associations, accumulated at proximal (Manfredonia Gulf), intermediate and distal shelf sectors. Spatial-temporal facies trajectories mainly reflect changes in fluxes of fine-grained, inorganic and organic particles at the seafloor. Major palaeoenvironmental shifts are paralleled by stratigraphic variations of Cr-Ni values, which represent effective provenance tracers for the Adriatic region. The correlation between the meiofauna content and trace-metal concentrations documents the link between the type of substrate (organic matter-OM and grain-size) and sediment provenance along the bathymetric profile and through time. After 6000 yr B.P., the gulf, partly sheltered by the Gargano Promontory, experienced the first increase in OM fluxes (transition from open-bay to prodelta). This turnaround occurred under the progressive change in sediment supply from southern Apennine source-rocks, poor in trace metals, to a mixed contribution including northern sources, enriched in chromium and nickel (mafic/ultramafic rocks of the Po River catchment) via the SSE-directed longshore drift. Alongside, prodelta clays in lateral transition to mud-belt deposits accumulated in the adjacent open shelf under the steady influence of the longshore drift. Finally, since ~2000 yr B.P. a pervasive subaqueous delta system developed across the study area in response to increased sediment load by Po + Apennine rivers, likely induced by enhanced anthropic pressure during Roman times. This study highlights the key role played by the sediment routing system, coastal morphology and human land-use on shelf facies patterns and eutrophication trends, even in areas hundreds of km away from the main fluvial mouths.

1. Introduction

Continental shelves represent a distinct and heterogeneous segment of the source-to-sink pathway for sediments, nutrients and dissolved elements from hinterland to basin(s) (Sømme et al., 2009; Zecchin and Catuneanu, 2013; Hanebuth et al., 2021; Pellegrini et al., 2021; Amorosi et al., 2022). Due to the interplay between river plumes, storms, currents and seafloor morphologies, a mosaic of depositional processes and environments commonly typifies worldwide shelves (Díaz et al., 1996; Mojtahid et al., 2009; de Araújo et al., 2018; Barbieri et al., 2019; Di Bella et al., 2021). Moving back through time, predicting depositional scenarios becomes even more difficult, as changes in global and local factors, including climate, relative sea-level (RSL), basin configuration, fluvial network and human land-use can promote variations in accommodation space, sediment supply and organic fluxes to the seafloor. This may lead to dramatic environmental changes, resulting in specific patterns of shallow-marine facies at different timescales (Owen and Lee, 2004; Liquete et al., 2010; Mendes et al., 2012; Catuneanu and Zecchin,

* Corresponding author.
E-mail address: veronica.rossi4@unibo.it (V. Rossi).

https://doi.org/10.1016/j.palaeo.2024.112055
Received 25 May 2023; Received in revised form 1 January 2024; Accepted 21 January 2024
Available online 26 January 2024

2013).

Holocene successions of modern shelves represent a valuable source of information about spatial-temporal dynamics of depositional environments and related forcing factors, owing to the high-resolution chronological framework guaranteed by radiocarbon dating and abundance of well-preserved proxies.

To robustly reconstruct past seafloor conditions from the stratigraphic record (e.g., water depth; quantity, quality and source of organic matter; nature of substrate; oxygenation), a multi-proxy approach, including palaeobiological (e.g., malacofauna, meiofauna, palynomorphs), geochemical (major and trace elements, isotopes) and/or physical (grain-size, sedimentary structures, magnetic susceptibility) indicators, is essential (e.g., Pascual et al., 2008; Schnedl et al., 2018; Mendes et al., 2020).

In the Mediterranean basin, several studies have integrated multivariate core data and high-resolution seismic profiles in a sequence-stratigraphic perspective, with the aim to assess lithofacies architecture, key surfaces and sediment budgets, in the frame of Milankovitch and sub-Milankovitch climate oscillations (Bellotti et al., 1994; Berné et al., 2007; Caruso et al., 2011; Di Bella et al., 2014; Zecchin et al., 2015; Amorosi et al., 2016; Tentori et al., 2018; Pellegrini et al., 2021).

Other works took advantage of high accumulation rates typical of prodelta lobes to highlight short-term (sub-millennial to multi-decadal) climate changes and their impact on circulation patterns and river(s) flood activity (Oldfield et al., 2003; Piva et al., 2008; Bassetti et al., 2016; Fanget et al., 2016; Pellegrini et al., 2023).

This study aims to furnish a comprehensive stratigraphic reconstruction of Holocene deposits along an across-shelf transect. The western Adriatic shelf and, in particular, the Manfredonia Gulf (SE Italy; Fig. 1) represent promising study sites, due to: *i)* the robust sequence-stratigraphic framework available (Maselli and Trincardi, 2013; De Santis et al., 2020a; Amorosi et al., 2023;); *ii)* deep knowledge of the subaqueous delta system, bottom morphology and oceanographic characteristics (Cattaneo et al., 2003, 2007; Spagnoli et al., 2008; Trincardi et al., 2014; Pellegrini et al., 2015), and *iii)* ample availability of sediment cores.

Our main objective is to reconstruct the spatial-temporal trajectories of shelf facies associations and sediment fluxes over the mid-late Holocene (last ~7000 years), by the integration of the meiofauna (benthic foraminifers and ostracods) and geochemical data from three cores (INV12–15; SI08–27; COS01–16) recovered at distinct depths (15 m, 30 m and 76 m) in the Manfredonia Gulf and the adjacent shelf (Fig. 1B).

Specific goal is to examine depositional dynamics and meiofauna-based eutrophication trends (i.e., organic enrichment; Gooday et al., 2009) at the seafloor far from the main Adriatic fluvial mouths (Fig. 1A), under highstand sea-level conditions.

2. Study site

2.1. Geological setting

The Adriatic Sea is a NW-SE elongated, epicontinental basin, belonging to the Alpine-Apennine and Dinarides-Hellenides foreland. It originated by the convergence between the European and African (Adria) plates (Doglioni, 1993; Boccaletti et al., 2011). The Manfredonia Gulf (MG) belongs to the seaward domain of the Bradanic Trough, the foredeep of the southern Apennines, which developed since the Early Pliocene (Tropeano et al., 2002). Up to the Early Pleistocene, shallow-marine carbonates and hemipelagic muds accumulated under high subsidence rates, due to the Adria subduction (Caldara et al., 2011). Thereafter, regional uplift (Doglioni et al., 1994) is recorded by a shallowing-upward succession partially exposed through terraces (De Santis et al., 2010, 2014).

Eastward, the Tavoliere Plain is fed by three rivers (Fig. 1B), from north to south: Candelaro, with the widest drainage basin (~2435 km^2), Cervaro (~625 km^2) and Carapelle (~1465 km^2).

The Adriatic shelf is gently dipping eastward (on average 0.07°), with a marked increase in bathymetric gradient around the 30 m-isobath, where an open shelf develops down to 150–160 m water depth (wd) (Maselli and Trincardi, 2013; Fig. 1B). Under a microtidal regime and the cyclonic circulation, the distribution of inorganic and organic particles is mainly controlled by waves and currents (e.g., Tesi et al., 2007; Turchetto et al., 2007). Two main currents flow from north to south along the western Adriatic shelf (Artegiani et al., 1997; Fig. 1): the surficial Western Adriatic Coastal Current (WACC) and the North Adriatic Dense Water current (NAdDW). Rounding the Gargano Promontory, which partly shelters the MG, the WACC induces the generation of a clockwise gyre allowing partial mixing with Ofanto River sediments (Spagnoli et al., 2008; Fig. 1A). Sediment distribution in the MG is controlled by the interaction between coastal morphology, local river inputs and sea currents (Spagnoli et al., 2008). Sands accumulated close to the coastline, down to the 20 m-isobath, whereas fine-grained sediments dominate the central and offshore areas, with the local occurrence of coralligenous build-ups (Spagnoli et al., 2010; Caldara et al., 2011).

2.2. Late Quaternary stratigraphy

Three cross-shelf erosional features that formed during the last glacial period are buried below the MG bottom, as revealed by high-resolution seismic profiles and core data. These river incisions correspond to palaeovalleys fed by the Candelaro (Manfredonia Incised Valley-MIV), Cervaro-Carapelle and Ofanto rivers (Maselli et al., 2014; De Santis and Caldara, 2016; De Santis et al., 2020a, 2020b; Amorosi et al., 2023).

The MIV has been extensively recognized down to 80 m wd, for an overall length of about 60 km, and its sedimentary infill is chronologically constrained to the present interglacial (Maselli and Trincardi, 2013). A deepening-upward succession of transgressive (fluvial and estuarine) facies overlain by highstand marine deposits has been documented. During the Early Holocene, RSL rise led to the development of a shallow-marine embayment that was rapidly filled around 7000 yr B.P. (Maselli et al., 2014). A muddy sediment body up to 35 m-thick characterizes the highstand portion, which represents the southernmost fringe of the Western Adriatic mud bank (Gargano subaqueous delta of Cattaneo et al., 2003; Fig. 1). Its uppermost portion includes the Little Ice Age (LIA) parasequence, identified across the Western Adriatic basin and dated around 450 yr B.P. (Pellegrini et al., 2021; Fig. 2).

2.3. Sediment provenance

Straight and short coastal rivers characterize the Apennine drainage of Apulia and adjacent areas. The MG and the Apulian offshore, in particular, are fed primarily by the Candelaro River, draining the Triassic-Miocene carbonate successions of the Gargano Promontory, and by Cervaro, Carapelle and Ofanto rivers, which flow from west to east through the siliciclastic formations exposed in the Southern Apennines (Fig. 1).

Sediment with remarkably different composition characterizes the Central Adriatic Sea: in this region, sediment supplied from Apennine rivers is mixed with sediment derived from the Po River and transported offshore Apulia through SSE-directed transport pathways by the powerful WACC (Fig. 1 - Cattaneo et al., 2003; Ravaioli et al., 2003; Spagnoli et al., 2008, 2014, 2021; Weltje and Brommer, 2011; Goudeau et al., 2013; Rovere et al., 2019).

The Po River is the largest single source of sediment to the Adriatic Sea. Due to the metamorphiclastic signature of its upper drainage basin, the Po River represents the main source of trace metals to the Western Adriatic Sea. Chromium and nickel, in particular, have been used to fingerprint source-rock composition from mafic/ultramafic successions of the Po River catchment against Apennine composition (Amorosi et al., 2002, 2014, 2022).

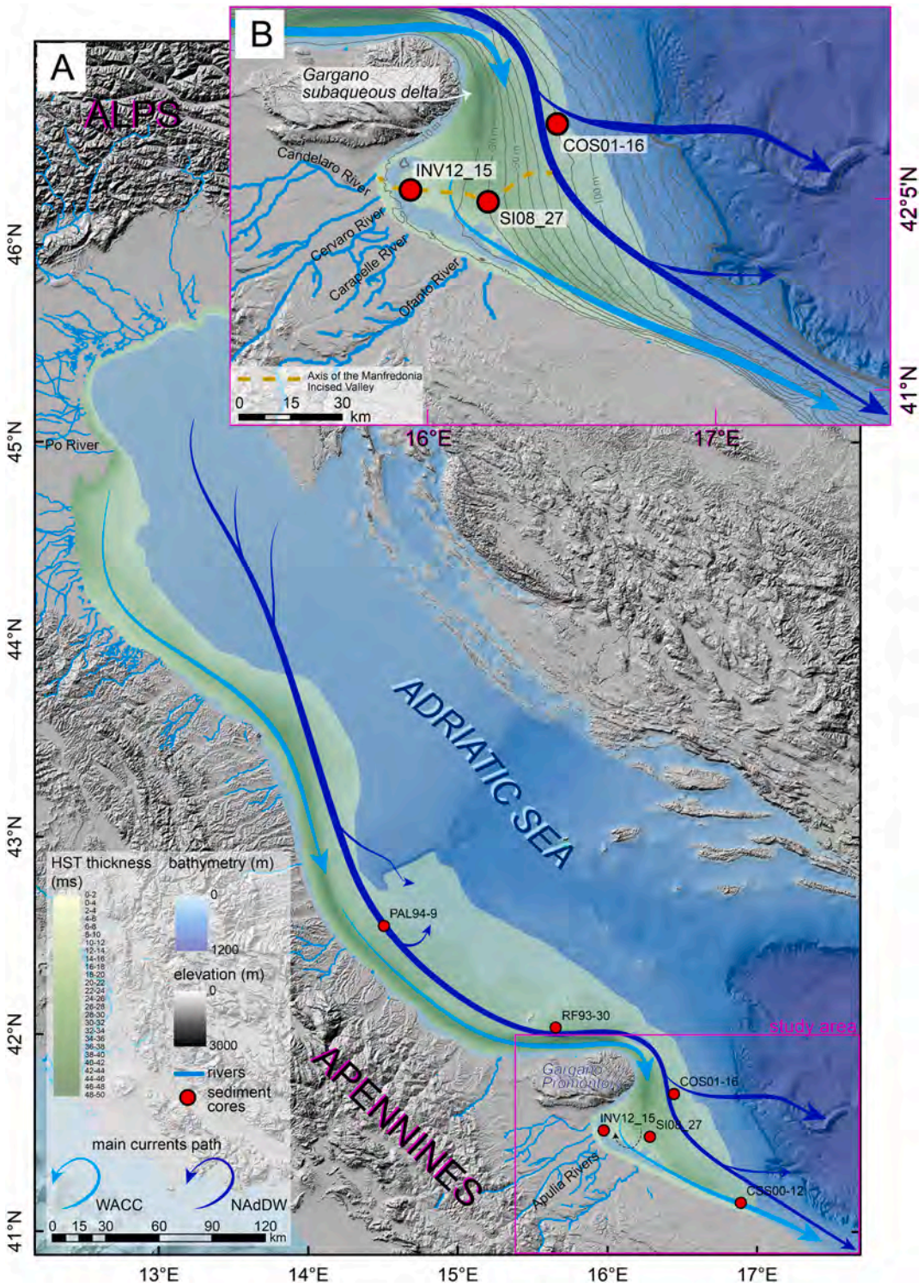

Fig. 1. Location map of the study area. A: Simplified geological and oceanographic setting of the Adriatic basin, with the thickness of the highstand mud bank highlighted by shades of green. Studied cores (INV12–15: 41°31′26.071″N-15°59′44.868″E, SI08–27: 41°30′53.188″N-16°18′9.019″E, COS01–16: 41°43′52.519″N-16°28′8.071″E) and other cores reported in Fig. 2 are also shown. WACC: Western Adriatic Coastal Current; NAdDW: North Adriatic Dense Water current. In the central portion of the Manfredonia Gulf (MG), the clockwise gyre is reported as a dotted line (after Spagnoli et al., 2008). B: The MG and the adjacent open shelf with the location of cores analyzed in this work. The contour of present-day bathymetry, the main currents and feeding rivers, and the Manfredonia palaeovalley axis are shown (after Spagnoli et al., 2008, 2010; Maselli et al., 2014). The Gargano subaqueous delta is highlighted by shades of green (after Cattaneo et al., 2003). (For interpretation of the references to color in this figure legend, the reader is referred to the web version of this article.)

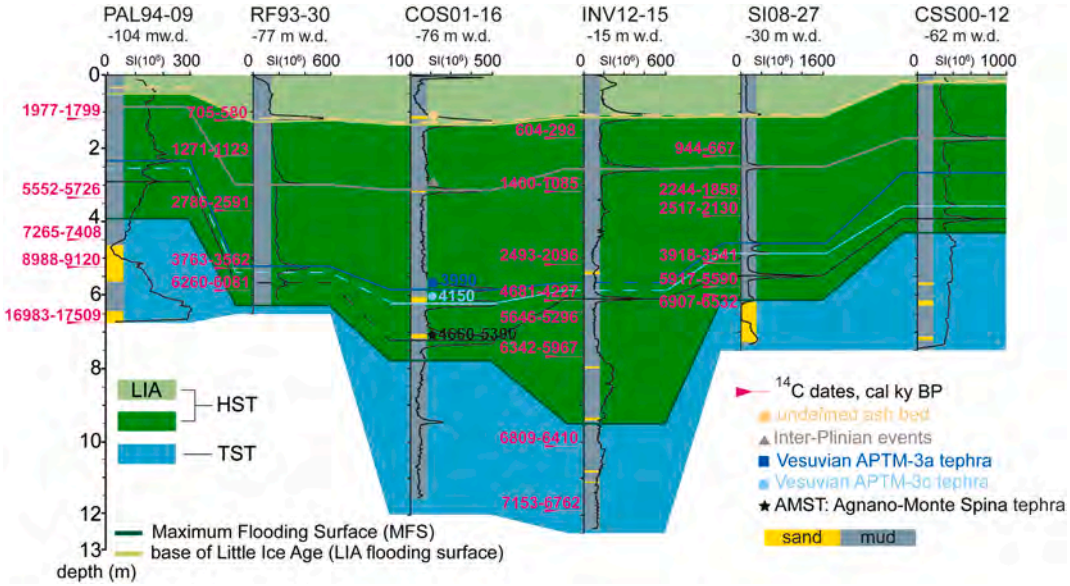

Fig. 2. Stratigraphic correlation panel through the central-south Adriatic shelf. The sequence stratigraphic interpretation of Holocene deposits (TST – Transgressive Systems Tract; HST – Highstand Systems Tract and MFS – Maximum Flooding Surface) is shown (Maselli et al., 2014; Pellegrini et al., 2015; Amorosi et al., 2016). Radiocarbon ages are from this study (core SI08–27) and from the literature (core PAL94–09 – Trincardi et al., 1996; core RF93–30 – Oldfield et al., 2003; core INV12–15 – Maselli et al., 2014). The chronological framework also took advantages from regional, seismic-stratigraphic correlations of tephra layers and magnetic susceptibility profiles (Table 2).

3. Material and methods

To assess millennial-scale facies patterns and concurrently track changes in sea-bottom conditions and sediment provenance, we coupled meiofauna and geochemical data of three cores collected along a dip-oriented, 50 km-long transect (INV12–15; SI08–27; COS01–16; Fig. 1B). These cores, collected via piston corer devices, were selected due to: *i)* their location in distinct bathymetric zones; *ii)* the predominance of mud containing abundant, well-preserved microfossils, and *iii)* the robust stratigraphic framework and lateral continuity of strata (Lowe et al., 2007; Maselli and Trincardi, 2013).

Cores INV12–15 (12.5 m-long) and SI08–27 (7 m-long) were retrieved from the inner shelf at water depths of 15 m and 30 m, respectively. Core COS01–16, 11.5 m long, was recovered at 76 m wd from the mid-outer shelf (Fig. 1B).

3.1. Meiofauna analysis and facies characterization

A comprehensive facies characterization of the cored succession was ensured by the quantitative analysis of the meiofauna: ostracods (OS) and benthic foraminifers (BF) are known to be excellent facies-environmental proxies, especially if jointly considered.

Seventy-one core samples were collected with a sampling rate of 2–3 samples/m (29, 19 and 23 samples from cores INV12–15, SI08–27 and COS01–16, respectively). For each sample, approximately 1–1.5 cm-thick slice of sediments was treated following the methodology reported in Barbieri et al. (2021). The fraction >125 μm was divided in aliquots and, when possible, a minimum of 300 well-preserved BF tests and 100 well-preserved OS valves (with carapaces considered as two valves) were counted. As for OS, both adult and juvenile valves with morphological characters sufficiently developed were counted. The raw dataset, the taxonomic list and reference literature are listed in Table S1. Palaeoecological inferences are mainly based on works by Breman (1975), Sgarrella and Moncharmont Zei (1993), Frezza and Carboni (2009), and Frezza and Di Bella (2015). Freshwater and brackish water ostracod taxa were removed from the dataset, being considered allochthonous.

To streamline the data, each matrix was treated prior to the application of multivariate analyses. The minimum threshold values of 150 tests and 20 valves were set for small samples (BF and OS, respectively). Taxa with similar ecological characteristics and *Ammonia* morphotypes (sensu Jorissen, 1988) were gathered up to reduce data dispersion.

Before applying ad hoc cut-off values and data transformation, counts were converted into relative percentages and matrices merged by groups (BF versus OS). Then, three different levels of cut-off (>5%; >4% and > 2% in at least one sample) were applied to remove rare taxa. Finally, we applied the Hellinger transformation (the square root of the relative abundance), as it effectively models ecological changes even within short environmental gradients (Legendre and Gallagher, 2001; Legendre and De Cáceres, 2013), and performed R-mode cluster analysis (CA) on each group. This latter allowed highlighting the main BF and OS assemblages, by the use of the unweighted pair-group method with arithmetic averaging (UPGMA) and the Correlation similarity index. The outputs obtained from matrices with different cut-off values are consistent, underlying the robustness of the assemblages. Here, we report the results deriving from the application of a 5% cut-off value.

The relative abundances of meiofauna assemblages were stratigraphically plotted along cored successions to identify environmental shifts and support detailed facies interpretation, which also benefited from: *i)* Q-mode CA outputs (i.e., groups of samples typified by specific meiofauna content), obtained via Correlation similarity index, and *ii)* lithological features (i.e., grain-size; presence/absence of malacofauna) reported in literature (Maselli and Trincardi, 2013; Maselli et al., 2014). Qualitative descriptions of the fossil content (mollusks, benthic foraminifers) available from core INV12–15 (Maselli et al., 2014) were not included in this work.

Detrended correspondence analysis (DCA) was also applied using the BF + OS matrix, with the aim to unravel facies turnover and related controlling factors within the stratigraphic record (Gliozzi and Grossi, 2008; Pascual et al., 2008; Laut et al., 2016; Rossi et al., 2018, 2021; Azzarone et al., 2020; Scarponi et al., 2022).

Multivariate analyses were performed with PAST ver. 4.04 (PAleontological STatistics; Hammer et al., 2001).

3.2. Geochemical analyses

A total of 76 samples (38 from core INV12–15, 16 from core SI08–27 and 22 from core COS01–16) were analyzed by X-ray fluorescence (XRF) for 11 major and 24 trace elements, at Bologna University. XRF analyses were integrated by XRF core scanning, performed at the Institute of Marine Science (CNR-ISMAR), Bologna. Samples were oven dried at 50 °C, powdered and homogenized in an agate mortar and analyzed using a Panalytical Axios 4000 spectrometer. The matrix correction methods of Franzini et al. (1972), Leoni and Saitta (1976), and Leoni et al. (1982) were adopted. The estimated precision and accuracy for trace-element determinations was 5%. For elements with low concentration (<10 ppm), the accuracy was 10%. In preparation for XRF core scanning, core surfaces were cleaned accurately and then scanned using an AVAATECH μXRF core scanner. Measurements were carried out using a Rhodium type anode set at 10, 30 and 50 kV with a resolution of 1 cm. The XRF spectral data were then converted to a record of net element intensities expressed as counts per second (cps). For chemostratigraphic interpretation, vertical trends in element abundance, rather than absolute values, were used.

In order to reduce the effect of hydraulic sorting on sediment composition (Garzanti et al., 2009), normalization of geochemical data was carried out using Al_2O_3 as a grain-size proxy (Covelli and Fontolan, 1997; Liaghati et al., 2003). The Ni/Al_2O_3 and Cr/Al_2O_3 ratios, in particular, have proved to be effective markers of sediment provenance for the Adriatic Sea area, enabling distinction between Apennine sources and sediment contribution from ultramafic (Alpine) source rocks (Amorosi et al., 2002, 2022; Greggio et al., 2018).

3.3. Cores dating

Fourteen AMS ^{14}C dates from mollusk shells, 8 from core INV12–15 and 6 from core SI08–27, are available (Table 1). Conventional ages were calibrated using the Marine20 curve (Heaton et al., 2020) and a reservoir age (Delta R) of 135.8 ± 40.8 yr (Piva et al., 2008). Ages are reported as calendar age Before Present (cal yr B.P.), with a 2-sigma error to better constrain the age model (Table 1).

A Bayesian age-depth model was constructed in the R environment using the "rbacon" package, as it produces reliable interpolations also in low-density dated successions affected by unsteady sedimentation regimes (Blaauw and Christen, 2011). To refine the model, which generates weighted mean age estimates every 5-cm intervals, changes in accumulation rates were supplied according to core stratigraphy (Table S2).

Further chronologic constraints derive from two types of basin-wide stratigraphic markers, identified through seismic-stratigraphic correlation (Table 2): *i)* tephra layers (Lowe et al., 2007), and *ii)* the base of the LIA parasequence (Piva et al., 2008). These data support the chronology of distal core COS01–16 (Table 2; Fig. 2).

Table 1
Radiocarbon dating. AMS ^{14}C ages used for the age-depth models..

Core	Core depth (m)	Dating material	Conventional age (yr B.P.)	Calibrated age (2_sigma cal yr B.P.)	References
INV12–15	11.91	Mollusk shell	6795 ± 35	7153–6762	Maselli et al., 2014
	10.02	Mollusk shell	6500 ± 40	6809–6410	Maselli et al., 2014
	7.78	Mollusk shell	6080 ± 40	6342–5967	Maselli et al., 2014
	6.45	Mollusk shell	5440 ± 40	5646–5296	Maselli et al., 2014
	6.16	Mollusk shell	4600 ± 40	4681–4227	Maselli et al., 2014
	5.28	Mollusk shell	2885 ± 30	2493–2096	Maselli et al., 2014
	2.64	Mollusk shell	1995 ± 30	1400–1085	Maselli et al., 2014
	1.70	Mollusk shell	1150 ± 40	604–298	Maselli et al., 2014
SI08–27	6.00	Mollusk shell	6590 ± 20	6907–6532	This study
	5.85	Mollusk shell	5710 ± 20	5917–5590	This study
	5.08	Mollusk shell	4060 ± 20	3918–3541	This study
	3.90	Mollusk shell	2910 ± 15	2517–2130	This study
	3.30	Mollusk shell	2680 ± 15	2244–1858	This study
	2.10	Mollusk shell	1560 ± 15	944–667	This study

4. Results

4.1. Meiofauna assemblages

The R-mode CA on the foraminiferal dataset led to the identification of five assemblages (BF1–5) and two singletons (*Ammonia beccarii* and *Bolivina*, *Brizalina* spp.), applying a cut-off level of 0.30 (Fig. 3A). Six ostracod assemblages (OS1–6) were obtained, instead, using a cut-off level of 0.20 (Fig. 3B). For each assemblage, the composition and ecological preferences of taxa are summarized below and in Table 3. Information about bottom conditions (grain-size, OM abundance) and water depth mainly derive from modern Adriatic databases (Breman, 1975; Bonaduce et al., 1975; Jorissen, 1987; Donnici and Serandrei Barbero, 2002; Barbieri et al., 2019). Concerning BF, special attention was paid to the ecological categories defined by Jorissen et al. (2018) based on OM gradients (i.e.: sensitive – indifferent – third-order to first-order opportunistic).

4.1.1. Benthic foraminifers

The BF1 assemblage shows the co-occurrence of indifferent *Reussella spinulosa* and opportunistic *Valvulineria bradyana*, both thriving on lower infralittoral to circalittoral muddy bottoms.

The BF2 assemblage groups several, mud-preferring taxa with a different degree of tolerance to oxygen deficiency and OM (from indifferent to third-order opportunistic), and commonly living within the circalittoral-bathyal range.

Table 2
Chronological markers identified within the studied cores and correlated at regional scale (see also Fig. 2).

Core	Core depth (m)	Type (*based on correlation)	Assigned age (yr B.P.)	References
INV12–15	6.00	*AMST tephra	4660–5390	Lowe et al., 2007; this study
	1.10	*base of the LIA	450	Piva et al., 2008; this study
SI08–27	5.50	*AMST tephra	4660–5390	Lowe et al., 2007; this study
	4.75	* Vesuvian APTM-3c tephra	4150	Lowe et al., 2007; this study
	4.55	* Vesuvian APTM-3a tephra	3990	Lowe et al., 2007; this study
	1.05	*base of the LIA	450	Piva et al., 2008; this study
COS01–16	7.15	AMST tephra	4660–5390	Lowe et al., 2007
	6.15	Vesuvian APTM-3c tephra	4150	Lowe et al., 2007
	5.75	Vesuvian APTM-3a tephra	3990	Lowe et al., 2007
	1.40	*base of the LIA	450	Piva et al., 2008; this study

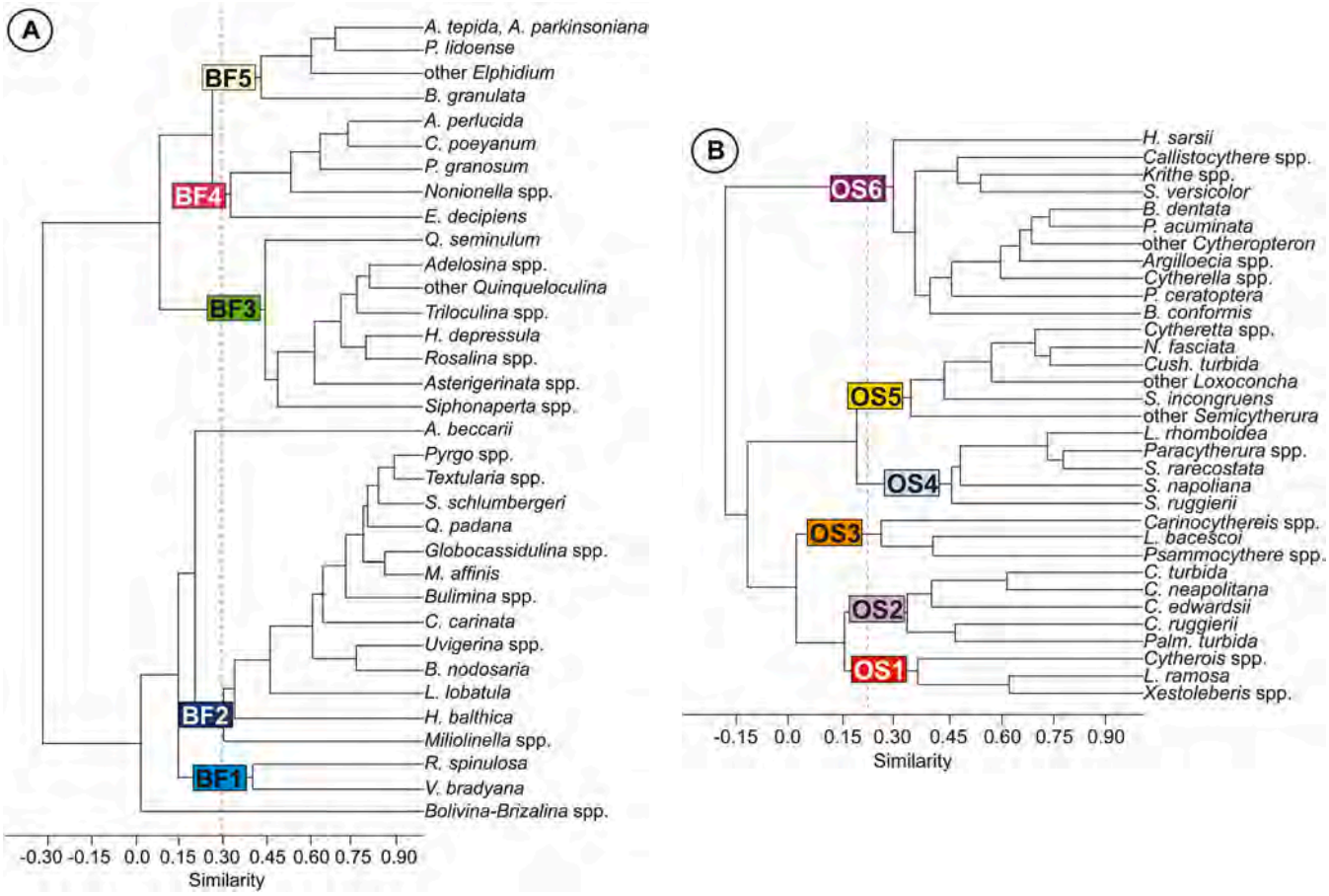

Fig. 3. Results of the R-mode cluster analysis performed on the meiofauna of cores INV12–15, SI08–27 and COS01–16 (Fig. 1B for location). A: Benthic foraminiferal assemblages (BF1–5) and two singletons. B: Ostracod assemblages (OS1–6). Dotted lines correspond to the cut-off levels.

Assemblages BF3-BF5 include taxa preferring infralittoral settings. BF3 is predominantly composed of Miliolids and hyaline epiphytic taxa thriving sandy bottoms subject to low OM fluxes. By contrast, BF4 groups mud-preferring opportunistic species, including *Aubignyna perlucida*, *Porosononion granosum* and *Cribroelphidium poeyanum,* plus indifferent *Elphidium decipiens*. The co-occurrence of opportunistic, indifferent and sensitive taxa proliferating on sand-mud substrates (*Ammonia tepida*, *Ammonia parkinsoniana*, *Porosononion lidoense*, *Buccella granulata*) typifies BF5.

4.1.2. Ostracods

The OS1 assemblage is composed of infralittoral taxa commonly thriving on sand-mud bottoms, such as opportunistic *Leptocythere ramosa* and phytal species belonging to *Xestoleberis* genus. Infralittoral-upper circalittoral taxa typify assemblages OS2 and OS3: OS2 groups several mud-preferring species, also including opportunistic *Palmoconcha turbida* and *Cytheridea neapolitana*, whereas OS3 taxa show tolerance to variable OM fluxes and heterogeneous granulometries (*Leptocythere bacescoi*, *Carinocythereis* spp.). Both OS4 and OS5 assemblages group infralittoral species commonly found on sandy substrates with low OM content; however, OS4 includes phytal species as *Loxoconcha* ex gr. *rhomboidea* and *Sagmocythere napoliana,* while typical nearshore taxa (e.g., *Cushmanidea turbida*) and ubiquitous *Semicytherura incongruens* characterize OS5. The OS6 assemblage groups several circalittoral-epibathyal and few infralittoral-circalittoral taxa (e.g., *Pterygocythereis ceratoptera*) preferring muddy bottoms and for the most part positively correlated with OM (e.g., *Henryhowella sarsii*, *Bosquetina dentata*, *Bairda conformis*, *Argilloecia* spp.).

4.2. Facies interpretation

4.2.1. Proximal sector (core INV12–15; wd ~15 m)

The 12.5 m-long succession, spanning the last ~7000 years, includes three, shallow-marine facies associations (Fig. 4).

- *Bay (12.5–7.5 m core depth)*

This facies association consists of 5 m-thick sandy muds, locally alternating with dm-thick muddy bedsets (Maselli et al., 2014). Samples (Q4–5 *plus* two singletons) show high percentages of assemblages BF3 (36–72%) and OS4 + OS5 (38–66%). Miliolids (mainly *Triloculina*, *Adelosina* and *Quinqueloculina* species), *L. rhomboidea* and *Semicytherura* species are the dominant taxa. The remaining part includes species belonging to BF4, BF5 (e.g., *C. poeyanum*, *A. tepida*, *A. parkinsoniana*) and OS1, OS3 (e.g., *L. ramosa*, *Carinocythereis* spp.). Within the uppermost 2 m (Q5), reduced amounts of OS4 + OS5 are locally recorded in favour of OS1 + OS3 or isolated peaks in OS2 (i.e., *C. neapolitana*; *P. turbida*) and OS6 (i.e., *P. ceratoptera*).

This facies is interpreted as an open-bay environment affected by wave activity, which favoured sandy bottoms and high availability of calcium carbonate. The OM fluxes via river plumes are generally scarce. Although discontinuous, an upward-increasing trend of OM is highlighted by ostracods, where OS1–3 taxa preferring muddy and organic-rich bottoms exhibit remarkable abundance.

- *Prodelta transition (7.5–5 m core depth)*

This facies association is characterized by 2.5 m-thick muddy

Table 3
Key features of the meiofauna assemblages (BF and OS clusters) and associated environmental interpretation. Although *Porosononion granosum* and *Porosononion lidoense* are now gathered in a single species (*P. granosum*; https://www.marinespecies.org), we prefer to keep them distinguished due to their distinct ecological distribution in the Adriatic Sea (e.g., Jorissen, 1987, 1988) and their different degree of opportunism (Jorissen et al., 2018). Infralittoral and circalittoral water-depth ranges refer to Sgarrella and Moncharmont Zei (1993): about <50 m and 50-200 m, respectively.

Label	Main taxa and ecological features	Palaeoenvironmental interpretation	References
BF1	*Reussella spinulosa* (sensitive), *Valvulineria bradyana* (second-order opportunist, tolerant to oxygen deficiency)	- Lower infralittoral-circalittoral - Muddy bottom - Moderate to high OM	Van Der Zwaan and Jorissen (1991), Sgarrella and Moncharmont Zei (1993), Frezza and Carboni (2009), Avnaim-Katav et al. (2015), Goineau et al. (2015), Aiello et al. (2018), Jorissen et al. (2018)
BF2	*Melonis affinis* (third-order opportunist, tolerant to oxygen deficiency), *Cassidulina carinata* (second-order opportunist), *Uvigerina mediterranea*, *Bigenerina nodosaria* (indifferent)	- Circalittoral - Muddy bottom - High OM	Jorissen (1987), Di Bella and Casieri (2011), Van Der Zwaan and Jorissen (1991), Frezza et al. (2012), Dessandier et al. (2016), Aiello et al. (2018), Jorissen et al. (2018)
BF3	*Asterigerinata*, *Rosalina*, *Siphonaperta*, *Adelosina* species (sensitive, epiphytic, positively correlated with sand), *Quinqueloculina seminulum* (third-order opportunist)	- Infralittoral - Sandy bottom - Low to moderate OM	Donnici and Serandrei Barbero (2002), Frezza and Carboni (2009), Barbieri et al. (2019)
BF4	*Aubignyna perlucida* and *Porosononion granosum* (third-order opportunist)	- Infralittoral - Muddy bottom - Moderate OM	Jorissen (1987), Van Der Zwaan and Jorissen (1991), Sgarrella and Moncharmont Zei (1993), Bellotti et al. (1994), Barbieri et al. (2019)
BF5	*Ammonia tepida* (second-order opportunist), *Ammonia parkinsoniana* (sensitive), *Porosononion lidoense* (indifferent)	- Infralittoral - Sand-mud bottom - Moderate OM	Frezza and Carboni (2009), Mojtahid et al. (2009), Ferraro et al. (2012), Goineau et al. (2015), Barbieri et al. (2019)
OS1	*Leptocythere ramosa* (positively correlated with OM), *Xestoleberis* species (phytal, positively correlated with sand)	- Infralittoral - Sand-mud bottom - Moderate OM	Colalongo (1969), Frezza and Di Bella (2015), Barbieri et al. (2019)
OS2	*Palmoconcha turbida* (positively correlated with OM, tolerant to oxygen deficiency), *Cytheridea neapolitana* (positively correlated with OM), *Cistacythereis turbida* (not tolerant to strongly eutrophic conditions)	- Infralittoral-upper circalittoral - Muddy bottom - Moderate to high OM	Bonaduce et al. (1975), Bodergat et al. (1998), Frezza and Di Bella (2015), Barbieri et al. (2019)
OS3	*Leptocythere bacescoi* (tolerant to variable OM and bottom grain-size), *Carinocythereis* species (positively correlated with OM)	- Infralittoral-upper circalittoral - Sand-mud bottom - Moderate OM	Athersuch et al. (1989), Montenegro and Pugliese (1996), Aiello et al. (2006), Barbieri et al. (2019)
OS4	*Loxoconcha rhomboidea* and *Sagmocythere napoliana* (phytal; negatively correlated with OM, positively correlated with sand), *Semicytherura ruggierii* (positively correlated with sand)	- Infralittoral - Sandy bottom - Low OM	Breman (1975), Barbieri et al. (2019)
OS5	*Neocytherideis fasciata*, *Cushmanidea turbida*, *Cytheretta* species (negatively correlated with OM)	- Infralittoral (nearshore) - Sandy bottom - Low OM	Breman (1975), Barbieri et al. (2019)
OS6	*Bosquetina dentata* and *Bairda conformis* (positively correlated with OM), *Argilloecia* and *Krithe* species (positively correlated with OM, tolerant to oxygen deficiency), *Pterygocythereis ceratoptera*	- Circalittoral - Muddy bottom - High OM	Bonaduce et al. (1975), Breman (1975), Aiello et al. (2015)

intervals, with rare sand layers (Maselli et al., 2014). Samples (Q1) show a foraminiferal fauna almost equally composed of assemblages BF4 + BF5 (~40–50%) and BF3 (~35–40%). The former group mostly includes *P. granosum*, *A. tepida*, *A. parkinsoniana*; the latter is dominated by *Triloculina* and *Adelosina* species. The ostracod fauna sees remarkable amounts (~70–80%) of assemblages OS1 + OS3 (mainly L. *ramosa*, *Xestoleberis* spp., *L. bacescoi*). From 6.5 m upwards, OS1 becomes highly dominant in concomitance with an increasing trend of OS2 + OS6 (mainly *Cistacythereis turbida*, *C. neapolitana*, *P. ceratopera*).

Sedimentological and palaeontological features point to a shallow-marine environment subject to a moderate, but continuous influence of river plumes, at the prodelta transition. An upward increase in river influence is suggested by increasing mud-preferring, opportunistic ostracod taxa.

- *Prodelta (< 5 m core depth)*

This facies association, which consists of 5 m-thick muds with low amounts (<5%) of sand (Maselli et al., 2014), includes samples belonging to clusters Q2–3. The meiofauna is abundant, with the exception of the uppermost sample (10 ostracod valves). Foraminifers are dominated by BF4 (~40–75%), particularly *A. perlucida*, *C. poeyanum* and *P. granosum*. Assemblages BF5 (17–28%) and, to a lesser extent (<20%), BF3 occur as secondary components. The uppermost meter shows an increase in BF4, especially *A. perlucida*, to the detriment of BF3. Ostracod assemblages OS1 + OS3 (mainly *L. ramosa* and L. *bacescoi*) strongly prevail, reaching ~50–80%. A minor change occurs around 3 m core depth, as the lowermost interval (Q2) displays the preeminence of OS3 and remarkable amounts (up to ~20–25%) of OS2 (*C. neapolitana*) and OS6 (*P. ceratopera*). Upsection (Q3), OS1 markedly increases (mostly L. *ramosa*).

These features reflect a prodelta environment steadily fed by river plumes that transported fine-grained inorganic and organic particles. A similar meiofauna is currently recorded along the Western Adriatic

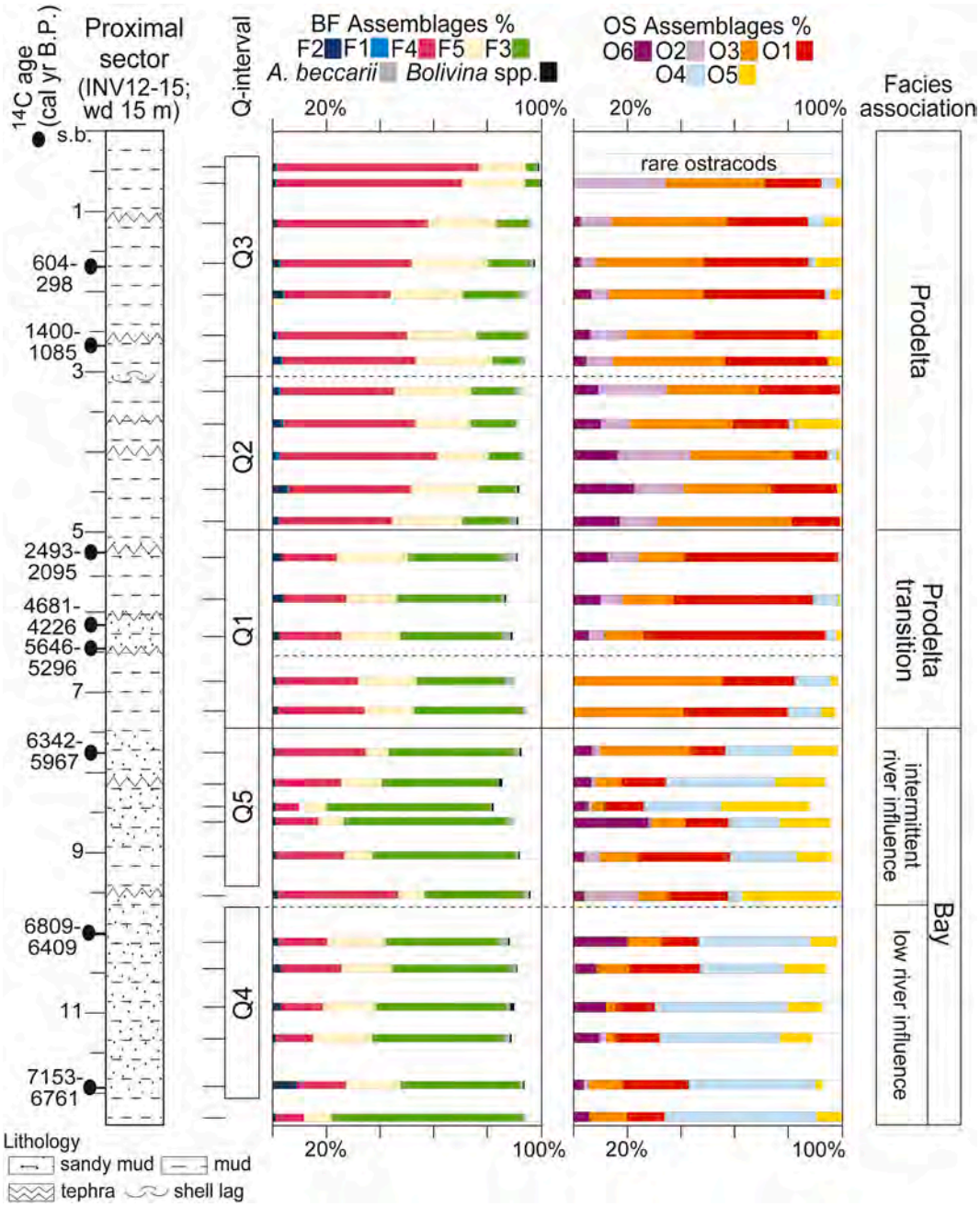

Fig. 4. Facies characterization, meiofauna stratigraphic trends and radiocarbon dating of the proximal sector (core INV12–15; Fig. 1B). Relative abundances of assemblages and Q-mode clusters both highlight major (solid line) and subtle (dotted line) changes in palaeoenvironmental conditions, as recorded along core stratigraphy.

coast, south of the Po Delta, around 10–20 m wd, where moderate OM enrichment is recorded (Barbieri et al., 2019). Changes in the ostracod fauna likely reflect subtle increase in river discharge, accompanied by a shallowing-upward trend, consistent with the scarcity of ostracods and the growth of *A. perlucida*.

4.2.2. Intermediate sector (core SI08–27; wd ~30 m)

The 7 m-long succession is composed of two facies associations; the upper stratigraphic interval spans the last ~7000 years (Fig. 5).

- *Transgressive barrier (7–6 m core depth)*

This facies association is a 1 m-thick, fining-upward (FU) succession of sands rich in shell fragments, with a shell lag at the core bottom (Maselli and Trincardi, 2013). The meiofauna is uniformly distributed throughout the interval (Q2), with a dominance of assemblages BF5 (~50–60%) and OS5 (~75–80%). The former mainly includes *Ammonia tepida*, *Ammonia parkinsoniana* accompanied by epiphytic taxa, such as *B. granulata* and *Elphidium* species. The latter is largely represented by *Cusch. turbida* and subordinate *S. incongruens*. Other assemblages are underrepresented, excluding BF3 that shows remarkable abundance (~20%) and the preeminence of miliolids, as *Triloculina* and *Siphonaperta* species.

Sedimentological features and the meiofauna point to a shoreface environment with vegetated bottom. The limited thickness, FU trend and basal shell lag point to a transgressive barrier.

- *Prodelta (<6 m core depth)*

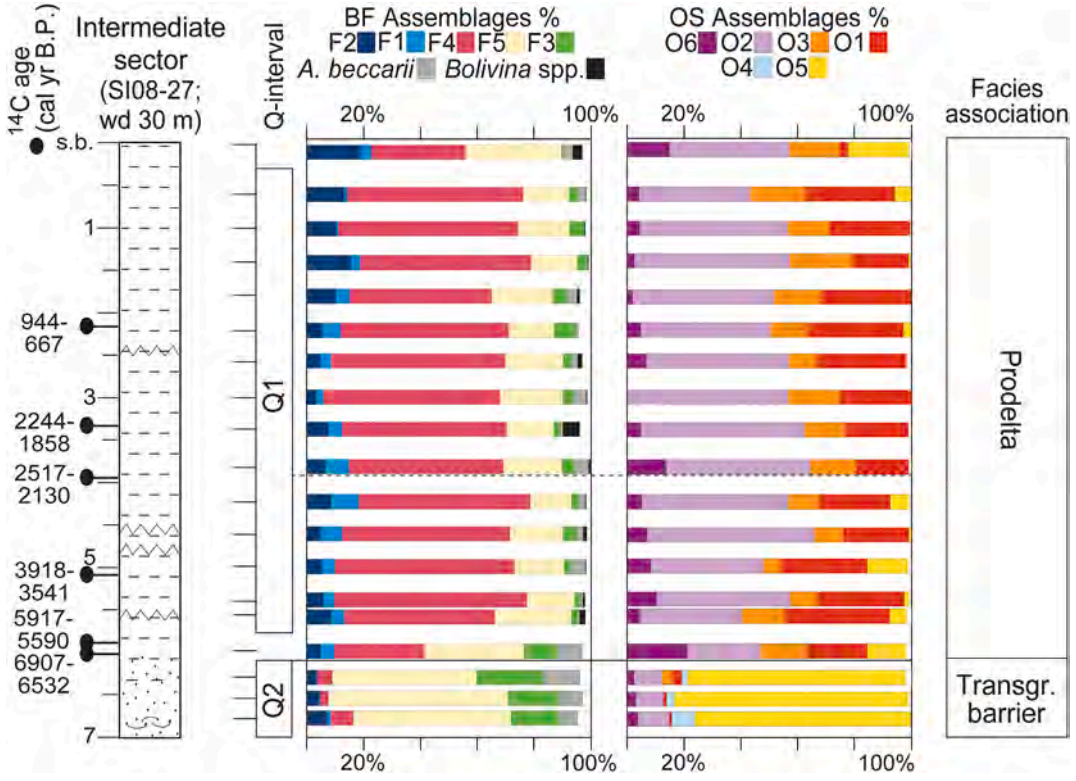

Fig. 5. Facies characterization, meiofauna stratigraphic trends and radiocarbon dating of the intermediate sector (core SI08–27; Fig. 1B). See Fig. 4, for lithological legend and Fig. 4 caption, for meiofauna data explanation.

A lithologically homogeneous muddy succession characterizes this 6 m-thick facies association (Maselli and Trincardi, 2013). Accordingly, the meiofauna is monotonous (Q1 + two singletons), with the steady dominance (~40–65%) of assemblages BF4 and OS2, and subordinate BF5 (~15–25%) and OS3 + OS1 (~35–50%). The most abundant species are *A. perlucida*, *P. granosum*, *C. poeyanum* and *C. neapolitana*. The uppermost singleton, collected at the modern sea bottom, displays only partial replacement of BF4 by BF5 (mainly *Ammonia* species) and OS1 by OS5 (mainly *S. incongruens*). By contrast, the singleton at the base contains a particular meiofauna including almost equal percentages of OS1–3, 5 and BF4, 5 assemblages. A subtle change in ostracod fauna also occurs around 4 m core depth, where OS5 taxa disappear.

The muddy lithology and meiofauna composition comparable to that living in the inner fringe of the modern Adriatic mud-belt (sensu Van Der Zwaan and Jorissen, 1991) point to a prodelta environment supplied by river plumes at water depths <25–30 m and moderately enriched in OM (Barbieri et al., 2019). An overall upward increase in river discharge is testified by changes in meiofauna composition.

4.2.3. Distal sector (core COS01–16; wd ~76 m)

Muddy deposits typify the 11.5 m-long succession, with the uppermost 7.5 m chronologically constrained to the last ~6000 years (Table 2). Despite lithologically homogeneous, vertical variations in meiofauna highlight the occurrence of three facies associations (Fig. 6).

- *Mid-outer shelf (11.5–9 m core depth)*

This facies association, which gathers Q4 samples *plus* one singleton, contains a rich meiofauna showing the co-dominance and upward increasing trends of BF2 (~40–60%) and OS6 (~35–60%) taxa, mainly represented by *Textularia* and *Bulimina* species, *Callistocythere* spp., *Krithe* spp. and *Sagmocythere versicolor*. The remaining part of the foraminiferal fauna basically corresponds to the indifferent *E. decipiens* (BF4) living in the Mediterranean at <100 m wd. OS2 (*C. neapolitana*, *Cytheropteron ruggierii*) and OS3 assemblages (*L. bacescoi*) are subordinate (about 20% and 20–35%, respectively). Low amounts (<10%) of *Semicytherura ruggierii* (OS4) are also observed.

These features indicate a mid-outer shelf environment, fed by moderate to high OM fluxes. An upward increase in OM is suggested by the growth of BF2 and OS6.

- *Mud-belt fringe (9–7.5 m core depth)*

This muddy interval, 1.5 m-thick, includes an abundant meiofauna almost entirely composed of BF2 and OS6 (~80–90% and ~ 85–95%, respectively; Q5). The most abundant taxa are *Uvigerina* species (~30–60%), mainly *U. mediterranea*, and *B. dentata* (~30–40%), with subordinate *Textularia*, *Bulimina*, *Argilloecia*, *Pterygocytheris* and *Cytheropteron* (mainly *C. monoceras*) species. Upsection, the genus *Cytherella* reaches ~10%.

This meiofauna points to a wd >70 m and high OM fluxes. Indeed, although classified as indifferent, the dominance of *U. mediterranea* suggests stressed conditions likely due to remarkable amounts of labile OM (Griveaud et al., 2010; Dessandier et al., 2016; Stalder et al., 2021). Ostracods tolerating a relatively low degree of oxygenation, such as *Argilloecia* and *Cytherella* species (Aiello et al., 2015; Angue Minto'o et al., 2015), point to periodic decrease in oxygen levels. Such conditions likely reflect the distal fringe of a mud-belt, where high OM accumulation at the seafloor occurs in response to the incoming suspended plume.

- *Mud-belt (<7.5 m core depth)*

Samples from this facies association show the steady dominance of assemblage BF2 (~50–85%), mainly *Textularia* and *Bulimina* species and, to a lesser extent, *M. affinis* (Q1–3). Low amounts (<15%) of BF4 and BF3 are encountered, and a peak in *V. bradyana* (BF1; ~10%) typifies the uppermost layer. Among ostracods, OS6 dominates (~55–75%) with high percentages of *B. dentata*, *P. ceratoptera* and *Callistocythere*

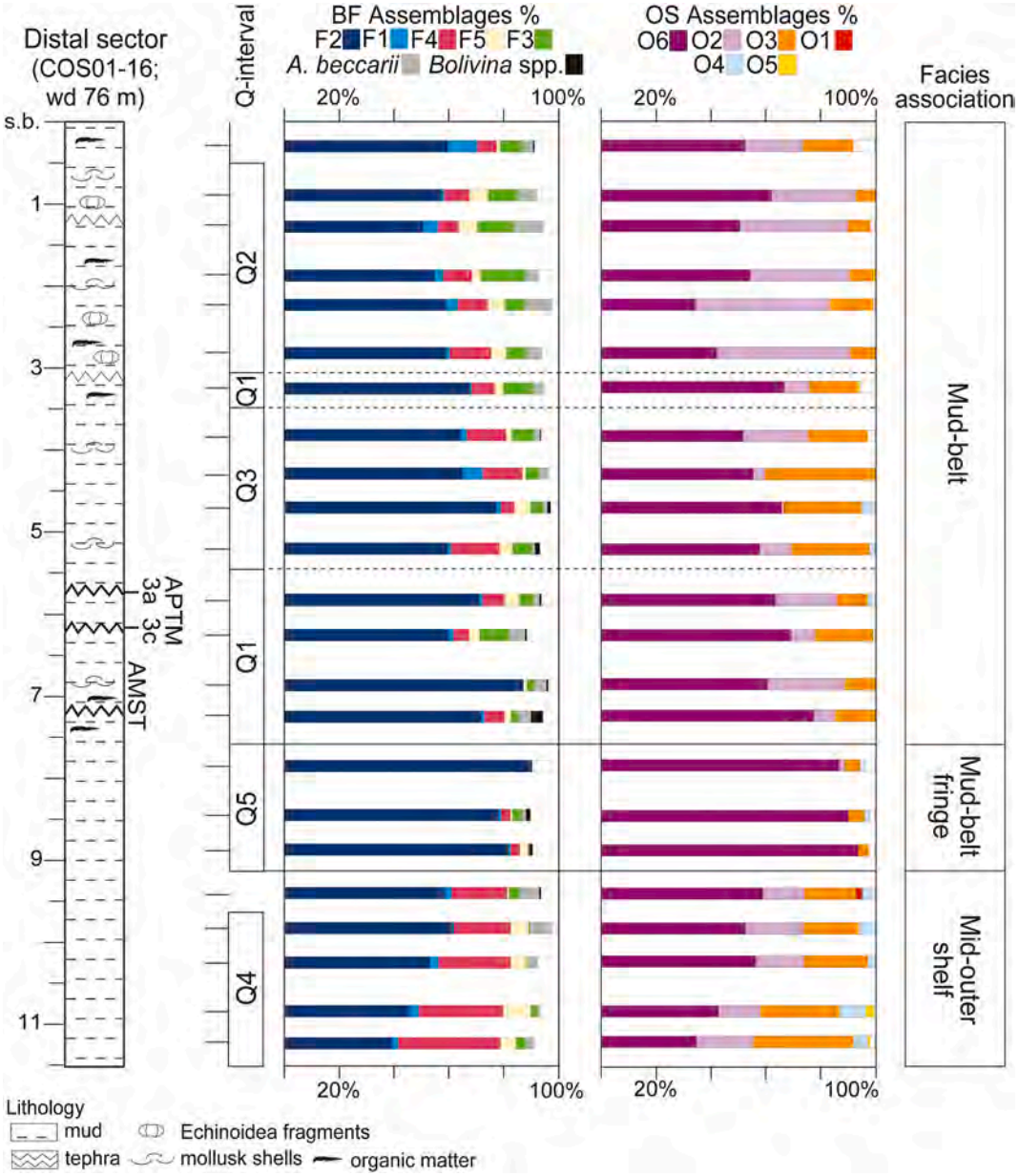

Fig. 6. Facies characterization and meiofauna stratigraphic trends of the distal sector (core COS01–16; Fig. 1B). See Fig. 4 caption, for meiofauna data explanation and Fig. 2 and Table 2 for tephra layers.

species in the lowermost 4.5 m (Q1, Q3). Upwards (Q2), OS6 is partly replaced by OS2 (~20–50%), almost entirely represented by opportunistic *C. neapolitana*. Within the middle portion of this interval (Q3) OS3, mainly L. *bacescoi*, reaches 30–40% accompanied by a peak (~10%) in *Cassidulina carinata* (BF2).

The meiofauna points to a shelf environment subject to high fluxes and accumulation of fine-grained particles (mud-belt). Remarkable amounts of *Bulimina* spp., *Melonis affinis* and, locally, *V. bradyana* suggest oxygen decrease (Bergamin et al., 1999; Fontanier et al., 2002). Although *C. carinata* can tolerate decreased oxygen levels, its peak likely documents high inputs of fresh phytodetritus/high quality OM (Morigi et al., 2005; Stalder et al., 2021). The upward decrease in OS6 suggests slightly decreasing bathymetry.

4.3. Indirect gradient analysis

The DCA plot shows a continuous distribution of BF and OS taxa along the major axis of variation (DC1 axis; Fig. 7), which accounts for ~43% of the data variance.

The turnover expressed along axis 1 is interpreted to reflect a complex environmental factor, overprinting a generally increasing bathymetric gradient, and corresponding to the type of substrate. By contrast, DC2 axis, which explains ~11% of the data variance, cannot be robustly related to any discernible parameters.

Infralittoral taxa thriving on sandy substrates and showing low tolerance to organic enrichment (assemblages BF3, OS4 and OS5; Fig. 7) attain the lowest DC1 scores on the left side of the plot (DC1 < 120–125). The right side, corresponding to the highest values of DC1 (>300), hosts circalittoral to bathyal taxa preferring organic-enriched muddy bottoms (assemblages BF2 and OS6; Fig. 7). In the middle DC1 portion, the distribution of taxa preferring variable amounts of mud and OM is discernible. Specifically, infralittoral species typical of mixed to muddy substrates moderately enriched in OM (BF4–5; OS1 and OS3) plot around 125–200 scores, while taxa thriving on infralittoral to circalittoral muds under moderate to high fluxes of OM attain values between ~200–300 (BF1, OS2 assemblages and BF2 and OS6 taxa also thriving

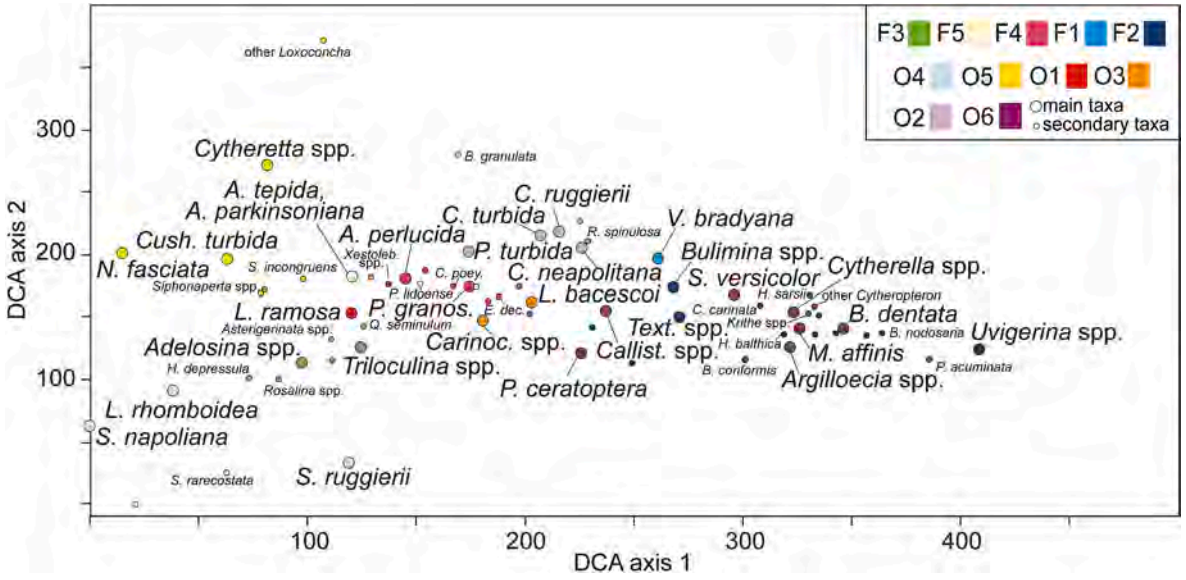

Fig. 7. DCA output reports for the total meiofauna dataset (DC1 variance: ~43%; DC2 variance: ~11%). Each color corresponds to a specific cluster/assemblage (see Figs. 4–6 for legend); BF singletons are in grey. The most abundant taxa are shown and key taxa are highlighted by big-sized circles. Samples are plotted in Fig. S2.

infralittoral settings; Fig. 7).

Within marine deposits, the proportion of mud and OM concentration are known to be interrelated, as mud is prone to be more organic-enriched than sand (Kennedy et al., 2002). Moreover, these physico-chemical parameters are commonly considered key drivers for meiofauna distribution on shelves, concurring to determine particular depositional environments at distinct bathymetric ranges (Pascual et al., 2008; Frezza and Carboni, 2009; Angue Minto'o et al., 2013; Frezza and Di Bella, 2015; Barbieri et al., 2019).

Accordingly, samples show a well-defined distribution in relation to water depth and sedimentology (Figs. 1, 4–6 and Fig. S1). Sandy-mud samples from the proximal sector (core INV12–15, ~12.5–6 m) and sands from intermediate water depths (core SI08–27, 7–6 m) plot at the left side (DC1 scores ⟨100−110). Muddy samples from both cores group in the middle along DC1 axis (scores ~115–215), while samples from the distal core (COS01–16) plot on the right side (scores >250).

4.4. Chemostratigraphy

The analysis of selected geochemical indices (Ni/Al_2O_3 and Cr/Al_2O_3) from 37 samples of core INV12–15, coupled with Ni counts from XRF scanning of the same core reveal consistent variations in trace-metal contents that reflect changes in sediment provenance (Fig. 8).

In its lower part (bay deposits with low to intermittent river influence), core INV12–15 typically exhibits relatively low Ni/Al_2O_3 and Cr/Al_2O_3 values (<3 and < 8, respectively), with small down-core variation (Fig. 8). In all core profiles, a prominent shift in sediment composition separates the lower interval from overlying, prodelta deposits (Fig. 8). Within the prodelta-transition facies association, around 6.00–6.50 m core depth, nickel and chromium exhibit progressively upward increasing levels, maximum values being recorded in the uppermost 2 m.

In general, trace-metal analysis reveals a strong control by source-rock lithology on sediment composition. In particular, low Ni and Cr levels in the lower part of core INV12–15 display strong affinity to sediment composition of modern Apulia rivers (Amorosi et al., 2022). Such low metal values reflect hinterland sediment supply from small, ophiolite-free Apennine drainages. On the other hand, distinctly higher nickel and chromium values in the overlying prodelta deposits denote an increasing proportional contribution of Alpine (Ni- and Cr-rich) material to the Adriatic coastal system (Amorosi et al., 2022).

Increasing Ni and Cr values upsection indicate a progressive change in the sediment routing system that is traceable at the basin scale. The overall compositional trend is consistent with meiofauna variations recorded by the benthic foraminifer and ostracod records (Fig. 4) and suggests a mixed signature of chiefly Apennine composition with a minor supply from northern sources (Po River) that could propagate downstream via the SSE-directed longshore drift.

4.5. Chronology and accumulation rates

In the proximal sector, the highest accumulation rates (~1 cm/yr) are associated to bay deposits, dated around 6800–6300 cal yr B.P. Distinctly decreasing values typify the prodelta transition environment (~0.1 cm/yr), with a marked drop around ~5300 cal yr B.P. (~0.05 cm/yr). Since ~2200 cal yr B.P., a rapid increase in net accumulation rates (~0.2 cm/yr) is associated to prodelta muds (Fig. 9A). No changes in accumulation rates are estimated for the LIA parasequence.

Above transgressive barrier sands, marine muds deposited in the intermediate sector show highly variable accumulation rates. About a millennium of very low sediment storage (~0.015 cm/yr) is estimated since ~6600 cal yr B.P. Afterwards, increasing accumulation rates are recorded (~0.06 cm/yr), with a major step around 2350 cal yr B.P. (~0.12 cm/yr in Fig. 9B). Even higher values are estimated for the LIA parasequence (~0.2 cm/yr).

Although accumulation rates for mid-outer shelf and mud-belt fringe deposits cannot be evaluated, a sediment storage of ~0.13 cm/yr typifies the mud-belt succession, up to the Vesuvian APTM-3a tephra layer (Q1 in Fig. 6; see also Fig. 2 and Table 2). Considering the Inter-Plinian events (Lowe et al., 2007) and the LIA flooding surface (Fig. 2), a substantially constant rate of sediment accumulation can be estimated up to ~450 yr B.P., followed by an increasing trend (~0.3 cm/yr).

5. Discussion

5.1. Mid-late Holocene facies patterns and forcing factors

The conceptual sketch of Fig. 10 illustrates the spatial-temporal relationships of Holocene facies associations across the MG, partly sheltered by the Gargano Promontory, and the adjacent open shelf. The integration with geochemical data and published RSL, climate records from the Adriatic area (Oldfield et al., 2003; Combourieu-Nebout et al.,

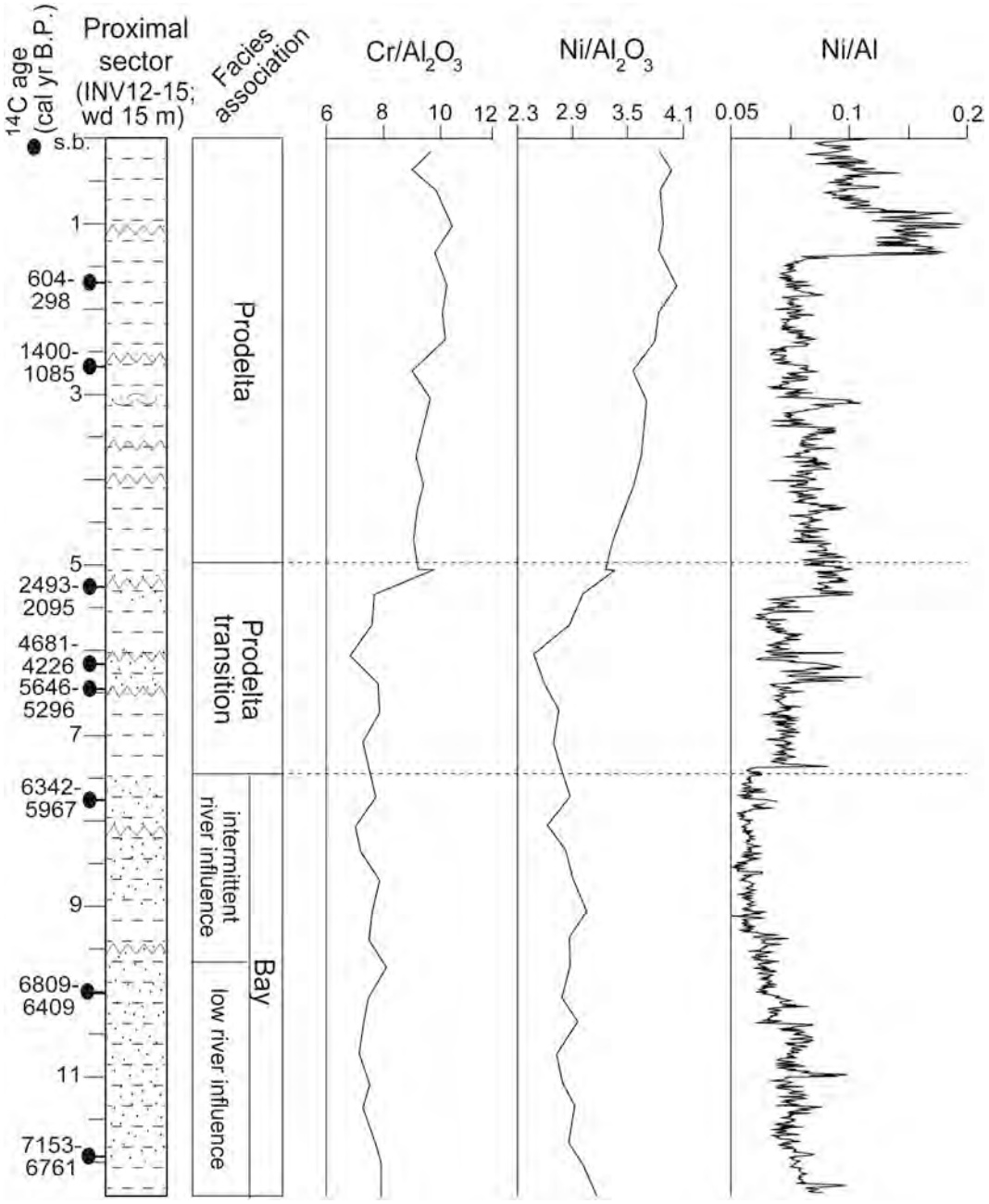

Fig. 8. Vertical profiles of selected geochemical indices and Ni counts from XRF scanning. See Fig. 4, for lithological legend.

2013; Vacchi et al., 2016, 2021) enable the assessment of the mechanisms that controlled sediment dispersal patterns and palaeoenvironments since ~7000 yr B.P. Four main stages are identified, with chronological boundaries around 6000, 2000 and 450 yr B.P.

The linear correlation between DC1 scores (Fig. 7) and key geochemical indices (Ni/Al_2O_3 and Cr/Al_2O_3) strongly supports the link between sea-bottom conditions and sediment provenance along the bathymetric profile and through time (Fig. 11).

5.1.1. 7000–6000 yr B.P. stage

Under increasing accommodation conditions, with an estimated RSL of ~5–6 m below the present (Vacchi et al., 2016), an open bay occupied the proximal area. Although sediment to the bay was supplied by the Apulia rivers, as testified by low Cr and Ni values (Figs. 8, 10–11), river plumes scarcely affected the sea bottom, which was colonized by taxa preferring low OM and sandy substrates as miliolids, belonging to *Adelosina*, *Quinqueloculina* and *Triloculina* genera, *Cush. turbida*, *L. rhomboidea* and *Semicytherura* species (BF3 and OS4–5; Table 3 and Fig. 4). Steadily high accumulation rates (~1 cm/yr) were locally fostered by the seafloor morphology (e.g., MIV depocentre; Fig. 1B) and, likely, by a homogeneous seasonal precipitation regime (Combourieu-Nebout et al., 2013).

In the intermediate sector, above relict coastal sands reasonably formed during the Early Holocene RSL jump (Vacchi et al., 2016), very slow accumulation (~0.015 cm/yr) of prodelta muds occurred. The co-dominance of opportunist and sensitive foraminifers (*P. granosum*, *A. tepida*, *A. parkinsoniana* and *B. granulata* from BF4–5; Table 3 and Fig. 5), along with an almost equal proportion of all ostracod assemblages (excluding OS4), point to a moderate OM enrichment. Stratigraphic condensation is coherent with the position of core SI08–27 on the MIV flank (Maselli et al., 2014; Fig. 1B) and on the fringe of the southward prograding Western Adriatic mud bank, beyond the Gargano

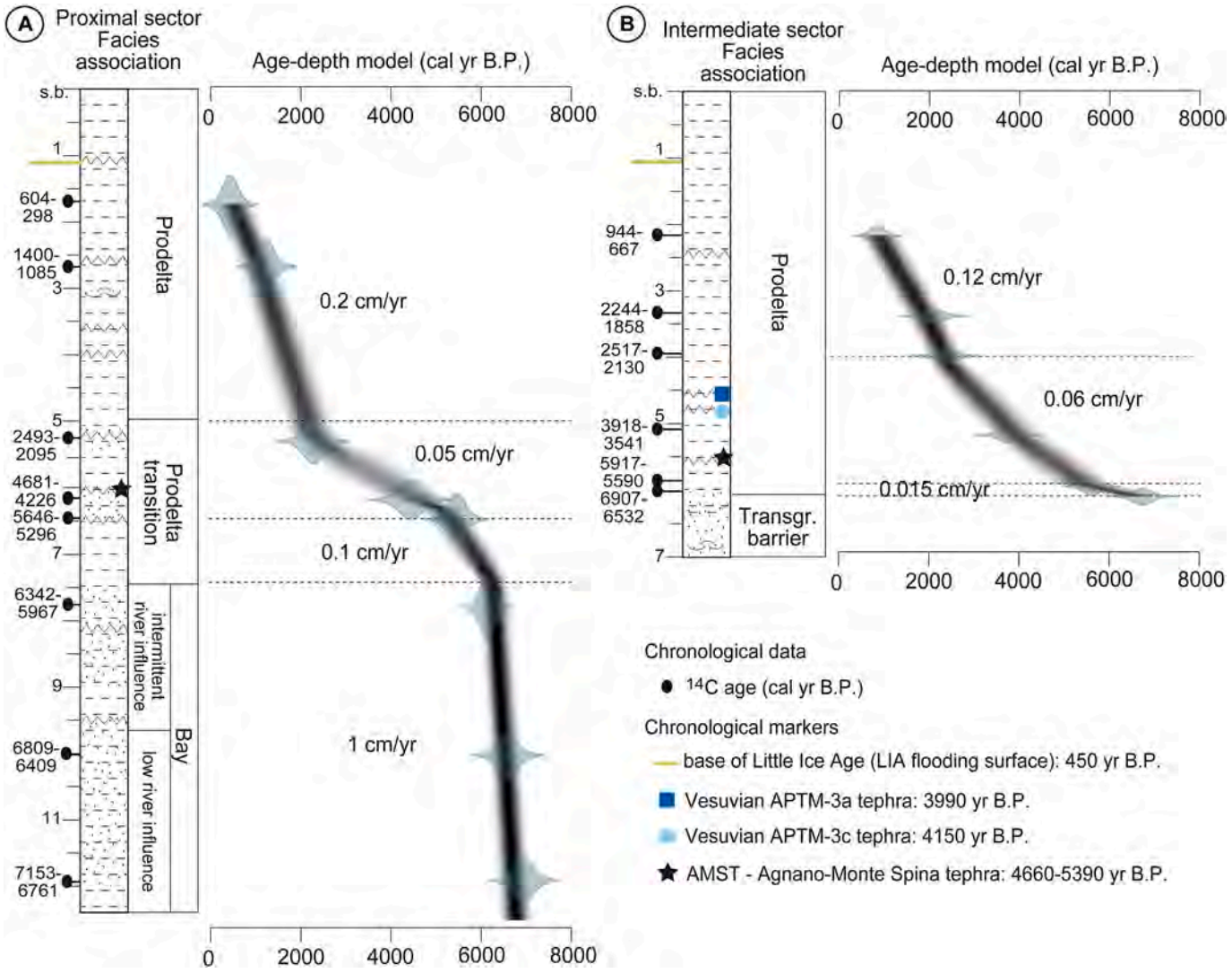

Fig. 9.

Promontory. Relatively high Cr and Ni values (Fig. 10) are indicative of a mixed sediment provenance, from the Apennines and the Po River (Amorosi et al., 2022). A similar geochemical fingerprint characterizes the distal sector, where muds enriched in labile OM (i.e., mud-belt fringe; Fig. 6) accumulated above mid-outer shelf deposits under the steady influence of the longshore drift.

5.1.2. 6000–2000 yr B.P. stage

Under reduced RSL rise (~2 m over 4000 years; Vacchi et al., 2016), a prodelta-transition environment replaced the bay in the proximal sector, marking the first significant increase in OM fluxes testified by the partial substitution of sensitive taxa (e.g., miliolids – BF3; *L. rhomboidea* – OS4) by opportunistic taxa (e.g., *P. granosum*, *L. ramosa,* and L. *bacescoi* – BF4 and OS1, 3; Table 3 and Fig. 4). Between ~6000–5000 yr B.P., Apulia rivers still acted as the main feeding source, as documented by low Cr and Ni values (Figs. 8, 10). Only since ~5000 yr B.P., longshore currents progressively increased their impact (higher Cr and Ni values; Fig. 8), building the progradation of the Adriatic mud bank within the MG (Fig. 10), along with the near disappearance of ostracods thriving sandy substrates poor in OM (OS4–5; Fig. 4). The incipient sediment bypassing of the Gargano Promontory was likely promoted by a phase of enhanced fluvial activity of the Po River, reasonably related to superposed climate (alternating drought–wet phases) and land-use factors (Amorosi et al., 2017; Rossi et al., 2021). Climate variability is known to influence fluvial regimes in terms of floods and sediment production–downstream delivery (e.g., Fletcher and Zielhofer, 2013; Benito et al., 2015), and the earliest widespread deforestation induced by transhumant pastoralism during the Eneolithic (Cremaschi and Nicosia, 2012; Bruno et al., 2015) could have increased river runoff. A drop in accumulation rates of over an order of magnitude (Fig. 9) was likely due to the MIV filling (Maselli et al., 2014). Similar rates (~0.06 cm/yr) typified the prodelta in its intermediate sector, where remarkable OM fluxes are recorded by the dominance of opportunistic species belonging to BF4 and OS1–2 (e.g., *P. granosum*, *C. poeyanum*, *A. perlucida*, *L. ramosa* and *C. neapolitana*; Table 3 and Fig. 5). This environment, as part of the main body of the Adriatic mud bank, passed distally to a mud-belt formed under high fluxes of fine-grained organic (dominance of opportunistic BF2 and OS6 species; Fig. 6) and inorganic (accumulation rate of ~0.13 cm/yr) particles.

5.1.3. 2000–450 yr B.P. stage

Since about 2000 yr B.P., under substantially stable RSL (Vacchi et al., 2021), a prodelta – mud-belt system supplied by longshore currents (high Cr and Ni values in Figs. 8, 10) grew across the study area, marking the pervasive establishment of the Gargano subaqueous delta (sensu Cattaneo et al., 2003; Fig. 10). Accumulation rates were high (~0.2 cm/yr to ~0.12–0.13 cm/yr), with the largest values in the proximal sector (Figs. 9–10). The establishment of widespread eutrophic

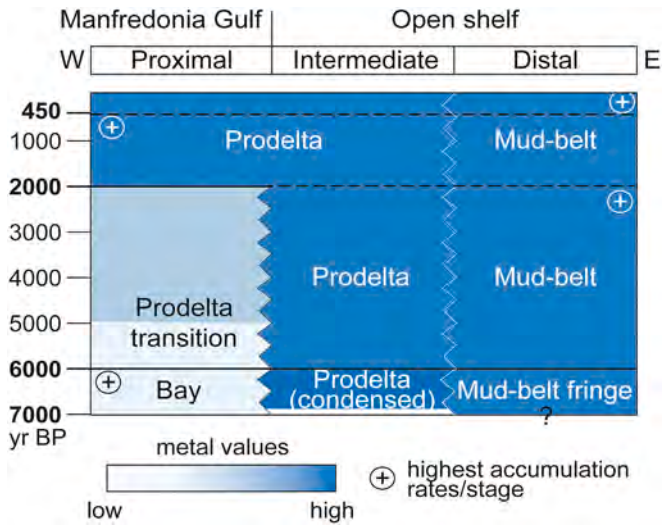

Fig. 10. South Adriatic facies distribution patterns along a 50 km-long bathymetric transect, over the last ~7000 yrs. B.P. The progressive eutrophication of MG, in response to progradation of the W Adriatic mud bank, is highlighted through time and space (from east to west). The facies characterization of proximal, intermediate and distal sectors is based on cores INV12–15, SI08–22 and COS01–16, respectively (cores location in Fig. 1); lateral facies relations are shown by wiggly lines. Sediment provenance, based on key geochemical indicators (Ni/Al_2O_3 and Cr/Al_2O_3), is highlighted as well as the shelf sector(s) typified by the maximum accumulation rates for each stage. Chronological constraints to palaeoenvironmental stages are in bold. Dotted lines reflect subtle changes between stages.

conditions is documented by the bathymetric distribution of the meiofauna (Figs. 4–6), which follows the ordination (DCA) results (Fig. 7). Specifically, *A. perlucida*, *L. bacescoi*, and L. *ramosa* (BF4, OS1, 3) characterized the proximal area, while *A. perlucida, P. granosum*, and *C. neapolitana* (BF4, OS2) thrived on the intermediate sector. The distal portion was typified by *Textularia* spp., *Bulimina* spp., *M. affinis*, *C. neapolitana*, and *B. dentata* (BF2, OS2, 6). This palaeoenvironmental shift occurred in response to increasing sediment supply by the longshore drift, coupled with a major growth phase of the Po Delta around 2000 yr B.P. (Oldfield et al., 2003; Maselli and Trincardi, 2013; Amorosi et al., 2019) related to enhanced anthropic pressure during the Roman Empire. Geoarchaeological studies (e.g., Mercuri et al., 2015; Marchesini and Marvelli, 2017) document a complex landscape, devoted to polyculture, pasture and water management, which fostered soil erosion in river catchments and downstream sediment transfer. In this context, coeval climate changes might have cooperated to increase river runoff (Bini et al., 2020).

5.1.4. *<450yr B.P. stage*

The lower limit of this stage corresponds to the onset of the LIA, a cooler climate oscillation characterized by increasing precipitation, storm and flood events (e.g., Glaser et al., 2010; Luterbacher et al., 2012; Sicre et al., 2016), also along the Western Adriatic (Pellegrini et al., 2021, 2023). This period saw an increase in urbanization and deforestation under growing populations, making it difficult to discern the role of climate from anthropic pressure on increasing sediment yields (Aucelli et al., 2004; Maselli and Trincardi, 2013; Anthony et al., 2014). Faint palaeoenvironmental changes are detected by the meiofauna in the MG. Specifically, the marked increase in BF4 and OS2 assemblages (mainly *A. perlucida*, *Palm. turbida* and *C. neapolitana*) documents further OM enrichment in the proximal sector (Figs. 4, 9; Table 3). Whereas, in the intermediate portion, a strengthening of bottom currents is suggested by increasing percentages of BF5 and OS5 species preferring sand-mud to sand bottoms (*A. tepida*, *A. parkinsoniana*, *S. incongruens* and *Cush. turbida*). Distally, no clear meiofauna signal is associated with the remarkable increase in accumulation rates (Figs. 6, 10).

5.2. *The progressive eutrophication of Manfredonia Gulf: A far-reaching effect of the Po-Adriatic sediment routing system*

The increase in the rate of OM supply is one of the major issues affecting coastal to shallow-marine environments, under the combined influence of natural and anthropogenic factors (e.g., Norbäck Ivarsson et al., 2019; Szymczak-Żyła et al., 2019). Over the last seven millennia, well-defined organic-enrichment trends typified the MG area, as highlighted by meiofauna-based facies patterns.

Since ~7000 yr B.P., the intermediate and distal shelf steadily hosted a river-influenced environment subject to moderate-to-high OM fluxes at the sea-bottom (i.e., prodelta–mud-belt system). By contrast, the proximal sector experienced the establishment of a prodelta only since ~2000 yr B.P. (Fig. 10), in response to the progradation of the Western Adriatic (Ni- and Cr-rich) mud bank. The Gargano Promontory acted as a natural barrier to SSE-directed sediment supply (Fig. 1). This headland delayed the modification of the bay into a muddy, OM-enriched environment, as recorded by the meiofauna turnover with opportunistic taxa strongly prevailing over the sensitive ones (Fig. 4).

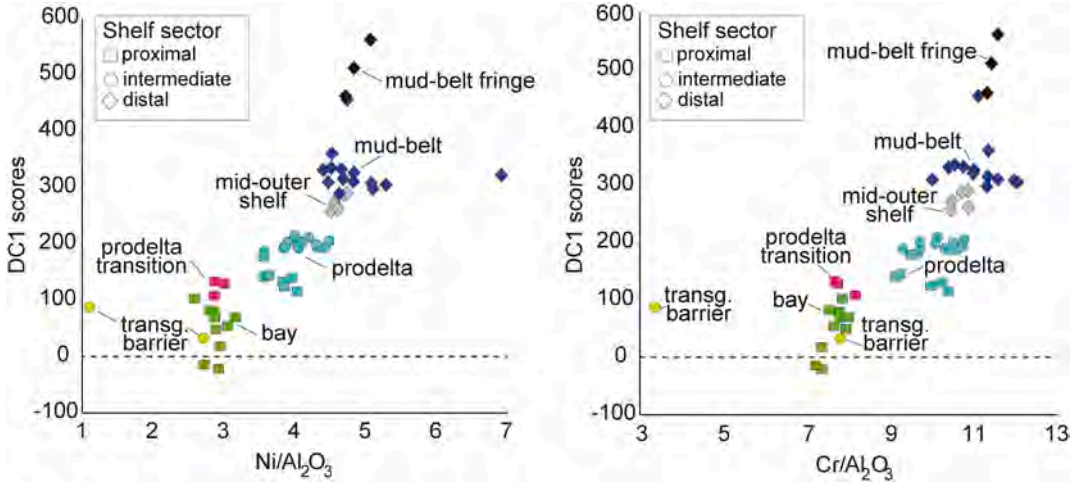

Fig. 11. Scatterplots of DC1 scores, representative of meiofauna palaeocommunities, versus Ni and Cr values from mid-late Holocene deposits of MG and the facing open shelf. Different colours highlight facies associations. The scatterplots reveal the positive correlation between sea-bottom conditions (OM and mud content) and sediment provenance.

Along the bathymetric gradient, the positive correlation between sea-bottom conditions (meiofauna DC1 scores in Fig. 7) and changes in sediment provenance is documented by the scatterplot of Fig. 11. Maximum metal enrichment ($Ni/Al_2O_3 > 4.4$, $Cr/Al_2O_3 > 10$) is observed in the distal sector (mud-belt samples), where the highest DC1 scores are also documented (dominant BF2 and OS6 taxa; Fig. 6). Prodelta samples show intermediate DC1 scores (dominant BF4–5 and OS1–3 taxa; Figs. 4, 5) and Ni/Al_2O_3 and Cr/Al_2O_3 values ranging between ~3.5–4.5 and ~ 9–11, respectively. On the other hand, prodelta-transition and bay samples, typified by taxa preferring low OM and sandy bottoms (BF3; OS4–5; Fig. 4), display low values of both indices.

The progressive eutrophication of the Manfredonia Gulf, thus, appears to have been governed by the Adriatic alongshore sediment dispersal concurrently with coastline morphology. Interestingly, the main increase in eutrophication south of the Gargano Promontory occurred under high sediment discharge by the Po River, with a further contribution by the Apennine rivers, associated to enhanced land-use during the Roman period (Maselli and Trincardi, 2013). This study thus demonstrates that human activities in river catchments, possibly superposed to climate oscillations, can fuel changes in the marine environment hundreds of km far from the main source of sediments, simply following basin circulation patterns.

6. Conclusions

Through a multi-proxy study of a Holocene succession from the southern Adriatic Sea, we examined the spatial-temporal dynamics of sediment fluxes and meiofauna communities from a shelf environment. The major conclusions are as follows:

- Five benthic foraminifer and six ostracod assemblages were identified across the shelf transect. Ordination results demonstrate that besides bathymetry, meiofauna distribution is driven by the type of substrate (proportion of fine-grained inorganic and organic particles).
- Quantitative meiofauna analysis is highly effective in identifying shelf facies associations and palaeoenvironmental trends, especially within apparently homogeneous muddy deposits.
- Geochemical fingerprinting reveals two separate sources of sediment: relatively low Ni and Cr contents typify Apulia rivers from the hinterland, whereas a Po River contribution is suggested by higher Ni and Cr contents via the Adriatic, SSE-directed longshore drift.
- Over the last ~7000 years, the stratigraphic-based integration of meiofauna and geochemical data documents four depositional-environmental stages, with chronological boundaries around 6000, 2000 and 450 yr B.P., along with the progressive eutrophication of the MG.
- Between 7000 and 6000 years, contrasting depositional environments (bay *versus* prodelta), accumulation rates and sediment provenance typified the proximal *versus* intermediate-distal sectors. The Adriatic sediment routing system, coastal morphology (barrier effect of Gargano Promontory), and seafloor palaeomorphology (MIV) acted as major controlling factors.
- After 6000 years, the bay turned progressively into a prodelta affected by longshore currents during a period of climate instability and first human land-use, under reduced RSL acceleration.
- Since ~2000 years, a subaqueous delta system supplied by longshore currents developed across the study area and entered the MG, documenting the spreading of the Adriatic mud bank in response to Roman activities. Subtle palaeoenvironmental changes occurred around 450 yr, under unstable climate conditions at the LIA onset.
- The positive correlation between the meiofauna and Cr-Ni values reveals the far-reaching effect of the Po River into the Adriatic sediment routing system and the long-term impact of human activities on shelf processes.

CRediT authorship contribution statement

Veronica Rossi: Conceptualization, Formal analysis, Investigation, Methodology, Visualization, Writing – original draft. **Irene Sammartino:** Formal analysis, Investigation, Methodology, Visualization, Writing – original draft, Writing – review & editing. **Claudio Pellegrini:** Investigation, Methodology, Visualization, Writing – review & editing. **Giulia Barbieri:** Formal analysis, Investigation, Writing – review & editing. **Chiara Teodoro:** Investigation. **Fabio Trincardi:** Supervision, Writing – review & editing. **Alessandro Amorosi:** Funding acquisition, Methodology, Project administration, Supervision, Writing – original draft, Writing – review & editing.

Declaration of competing interest

The authors declare that they have no known competing financial interests or personal relationships that could have appeared to influence the work reported in this paper.

Supplementary data to this article can be found online at https://doi.org/10.1016/j.palaeo.2024.112055.

Data availability

Raw data are available as Supplementary Material (Table S1)

Acknowledgments

We thank three anonymous reviewers for their constructive comments and suggestions. This work was supported by the Italian Ministry of University and Research under the PRIN 2017 program, project number 2017ASZAKJ “The Po-Adriatic Source-to-Sink system (PASS): from modern sedimentary processes to millennial-scale stratigraphic architecture”, grant to Alessandro Amorosi. We thank Marco Cacciari for the support with the age-depth models.

References

Aiello, G., Barra, D., Coppa, M.G., Valente, A., Zeni, F., 2006. Recent infralittoral Foraminiferida and Ostracoda from the Porto Cesareo Lagoon (Ionian Sea, Mediterranean). Boll. Soc. Paleontol. Ital. 45 (1), 1–14.

Aiello, G., Barra, D., Parisi, R., 2015. Lower–Middle Pleistocene ostracod assemblages from the Montalbano Jonico section (Basilicata, Southern Italy). Quat. Int. 383, 47–73.

Aiello, G., Barra, D., Parisi, R., Isaia, R., Marturano, A., 2018. Holocene benthic foraminiferal and ostracod assemblages in a paleo-hydrothermal vent system of Campi Flegrei (Campania, South Italy). Palaeontol. Electron. 21.3.41A, 1–71. https://doi.org/10.26879/835.

Amorosi, A., Centineo, M.C., Dinelli, E., Lucchini, F., Tateo, F., 2002. Geochemical and mineralogical variations as indicators of provenance changes in late Quaternary deposits of SE Po Plain. Sediment. Geol. 151 (3–4), 273–292. https://doi.org/10.1016/S0037-0738(01)00261-5.

Amorosi, A., Guermandi, M., Marchi, N., Sammartino, I., 2014. Fingerprinting sedimentary and soil units by their natural metal contents: a new approach to assess metal contamination. Sci. Total Environ. 500, 361–372.

Amorosi, A., Maselli, V., Trincardi, F., 2016. Onshore to offshore anatomy of a late Quaternary source-to-sink system (Po Plain-Adriatic Sea, Italy). Earth Sci. Rev. 153, 212–237.

Amorosi, A., Bruno, L., Campo, B., Morelli, A., Rossi, V., Scarponi, D., Hong, W., Bohacs, K.M., Drexler, T.M., 2017. Global sea-level control on local parasequence architecture from the Holocene record of the Po Plain, Italy. Mar. Pet. Geol. 87, 99–111.

Amorosi, A., Barbieri, G., Bruno, L., Campo, B., Drexler, T.M., Hong, W., Rossi, V., Sammartino, I., Scarponi, D., Vaiani, S.C., 2019. Three-fold nature of coastal progradation during the Holocene eustatic highstand, Po Plain, Italy–close correspondence of stratal character with distribution patterns. Sedimentology 66, 3029–3052.

Amorosi, A., Sammartino, I., Dinelli, E., Campo, B., Guercia, T., Trincardi, F., Pellegrini, C., 2022. Provenance and sediment dispersal in the Po-Adriatic source-to-sink system unraveled by bulk-sediment geochemistry and its linkage to catchment geology. Earth Sci. Rev. 234, 104202 https://doi.org/10.1016/j.earscirev.2022.104202.

Amorosi, A., Bruno, L., Caldara, M., Campo, B., Cau, S., De Santis, V., Di Martino, A., Hong, W., Lucci, G., Pellegrini, C., Rossi, V., Sammartino, I., Vaiani, S.C., 2023. Late Quaternary sedimentary record of estuarine incised-valley filling and interfluve

flooding: the Manfredonia paleovalley system (southern Italy). Mar. Pet. Geol. 147, 105975 https://doi.org/10.1016/j.marpetgeo.2022.105975.
Angue Minto'o, C.M., Bassetti, M.-A., Jouet, G., Toucanne, S., 2013. Distribution of modern ostracoda and benthic foraminifera from the Golo margin (East-Corsica). Rev. Paléobiol. 32 (2), 607–628.
Angue Minto'o, C.A., Bassetti, M.A., Morigi, C., Ducassou, E., Toucanne, S., Jouet, G., Mulder, T., 2015. Levantine intermediate water hydrodynamic and bottom water ventilation in the northern Tyrrhenian Sea over the past 56,000 years: new insights from benthic foraminifera and ostracods. Quat. Int. 357, 295–313.
Anthony, E.J., Marriner, N., Morhange, C., 2014. Human influence and the changing geomorphology of Mediterranean deltas and coasts over the last 6000years: from progradation to destruction phase? Earth Sci. Rev. 139, 336–361. https://doi.org/10.1016/j.earscirev.2014.10.003.
Artegiani, A., Paschini, E., Russo, A., Bregant, D., Raicich, F., Pinardi, N., 1997. The Adriatic Sea general circulation. Part II: baroclinic circulation structure. J. Phys. Oceanogr. 27 (8), 1515–1532.
Athersuch, J., Horne, D.J., Whittaker, J.E., 1989. Marine and Brackish Water Ostracods, Synopses of the British Fauna (New Series). Brill E.J, Leiden (345 pp).
Aucelli, P.P.C., Faillace, P.I., Pellegrino, P., Rosskopf, C.M., Scapillati, N., 2004. L'evoluzione recente della costa molisana (Italia meridionale). Il Quaternario Italian J. Quat. Sci. 17 (1), 21–31.
Avnaim-Katav, S., Hyams-Kaphzan, O., Milker, Y., Almogi-Labin, A., 2015. Bathymetric zonation of modern shelf benthic foraminifera in the Levantine Basin, eastern Mediterranean Sea. J. Sea Res. 99, 97–106.
Azzarone, M., Barbieri, G., Rossi, V., Gamberi, F., Trincardi, F., Scarponi, D., 2020. Linking benthic fauna and seismic facies to improve stratigraphic reconstructions: the case of the Mid-Adriatic deep since the late glacial period (Central Adriatic Sea). Boll. Soc. Paleontol. Ital. 59, 9–23. https://doi.org/10.4435/BSPI.2020.03.
Barbieri, G., Rossi, V., Vaiani, S.C., Horton, B.P., 2019. Benthic ostracoda and foraminifera from the North Adriatic Sea (Italy, Mediterranean Sea): a proxy for the depositional characterisation of river-influenced shelves. Mar. Micropaleontol. 153, 101772 https://doi.org/10.1016/j.marmicro.2019.101772.
Barbieri, G., Rossi, V., Vaiani, S.C., Dasgupta, U., Amorosi, A., 2021. Quantitative paleoecology in shallow-marine settings: the value of ostracods and foraminifers from the Holocene North Adriatic record. Palaeogeogr. Palaeoclimatol. Palaeoecol. 572, 110408 https://doi.org/10.1016/j.palaeo.2021.110408.
Bassetti, M.-A., Berné, S., Sicre, M.-A., Dennielou, B., Alonso, Y., Buscail, R., Jalali, B., Hebert, B., Menniti, C., 2016. Holocene hydrological changes in the Rhône River (NW Mediterranean) as recorded in the marine mud belt. Clim. Past 12, 1539–1553. https://doi.org/10.5194/cp-12-1539-2016.
Bellotti, P., Carboni, M.G., Valeri, P., Di Bella, L., Palagi, I., 1994. Benthic foraminiferal assemblages in the depositional sequence of the Tiber Delta. Boll. Soc. Paleontol. Ital. 2, 29–40.
Benito, G., Macklin, M.G., Panin, A., Fontana, A., Jones, A.F., Machado, M.J., Matlakhova, E., Mozzi, P., Zielhofer, C., 2015. Recurring flood distribution patterns related to short-term Holocene climatic variability. Sci. Rep. 5, 16398. https://doi.org/10.1038/srep16398.
Bergamin, L., Di Bella, L., Carboni, M.G., 1999. *Valvulineria bradyana* (Fornasini) in organic-matter enriched environment (Ombrone River mouth, Central Italy). Il Quaternario Italian J. Quat. Sci. 12 (1), 51–56.
Berné, S., Jouet, G., Bassetti, M.A., Dennielou, B., Taviani, M., 2007. Late Glacial to Preboreal Sea-level rise recorded by the Rhône deltaic system (NW Mediterranean). Mar. Geol. 245, 65–88. https://doi.org/10.1016/j.margeo.2007.07.006.
Bini, M., Zanchetta, G., Regattieri, E., Isola, I., Drysdale, R.N., Fabiani, F., Genovesi, S., Hellstrom, J.C., 2020. Hydrological changes during the Roman Climatic Optimum in northern Tuscany (Central Italy) as evidenced by speleothem records and archaeological data. J. Quat. Sci. 35, 791–802. https://doi.org/10.1002/jqs.3224.
Blaauw, M., Christen, J.A., 2011. Flexible paleoclimate age-depth models using an autoregressive gamma process. Bayesian Anal. 6, 457–474.
Boccaletti, M., Corti, G., Martelli, L., 2011. Recent and active tectonics of the external zone of the Northern Apennines (Italy). Int. J. Earth Sci. 100, 1331–1348. https://doi.org/10.1007/s00531-010-0545-y.
Bodergat, A.M., Ikeya, N., Irzi, Z., 1998. Domestic and industrial pollution: use of ostracods (Crustacea) as sentinels in the marine coastal environment. J. Rech. Oceanogr. 23, 139–144.
Bonaduce, G., Ciampo, G., Masoli, M., 1975. Distribution of Ostracoda in the Adriatic Sea. Pubblicazioni della Stazione Zoologica di Napoli. Olschki L. S, Napoli, Italy.
Breman, E., 1975. The Distribution of Ostracodes in the Bottom Sediments of the Adriatic Sea. PhD Thesis,. Free University of Amsterdam.
Bruno, L., Amorosi, A., Severi, P., Bartolomei, P., 2015. High-frequency depositional cycles within the late Quaternary alluvial succession of Reno River (northern Italy). Ital. J. Geosci. 134 (2), 339–354.
Caldara, M., Capolongo, D., del Gaudio, V., de Santis, V., Pennetta, L., Maiorano, P., Simone, O., Vitale, G., 2011. Note Illustrative Della Carta Geologica d'Italia Alla Scala 1:50.000, Foglio 422 'Cerignola'. Istituto Superiore per la Protezione e la ricerca Ambientale, Roma (96 pp).
Caruso, A., Cosentino, C., Pierre, C., Sulli, A., 2011. Sea-level changes during the last 41,000 years in the outer shelf of the southern Tyrrhenian Sea: evidence from benthic foraminifera and seismostratigraphic analysis. Quat. Int. 232, 122–131.
Cattaneo, A., Correggiari, A., Langone, L., Trincardi, F., 2003. The late-Holocene Gargano subaqueous delta, Adriatic shelf: sediment pathways and supply fuctuations. Mar. Geol. 193, 61–91.
Cattaneo, A., Trincardi, F., Asioli, A., Correggiari, A., 2007. The Western Adriatic shelf clinoform: energy-limited bottomset. Cont. Shelf Res. 27, 506–525. https://doi.org/10.1016/j.csr.2006.11.013.
Catuneanu, O., Zecchin, M., 2013. High-resolution sequence stratigraphy of clastic shelves II: Controls on sequence development. Mar. Pet. Geol. 39, 26–38.
Colalongo, M.L., 1969. Ricerche sugli Ostracodi nei fondali antistanti il delta del Po. Giorn. Geol. 36, 335–362.
Combourieu-Nebout, N., Peyron, O., Bout-Roumazeilles, V., Goring, S., Dormoy, I., Joannin, S., Sadori, L., Siani, G., Magny, M., 2013. Holocene vegetation and climate changes in the Central Mediterranean inferred from a high-resolution marine pollen record (Adriatic Sea). Clim. Past 9, 2023–2042.
Covelli, S., Fontolan, G., 1997. Application of a normalization procedure in determining regional geochemical baselines. Environ. Geol. 30, 34–45.
Cremaschi, M., Nicosia, C., 2012. Sub-Boreal aggradation along the Apennine margine of the Central Po Plain: geomorphological and geoarchaeological aspects. Géomorphologie 2, 155–174.
de Araújo, H.A.B., Dominguez, J.M.L., Machado, A.D.J., de Araújo, N., Rangel, A.G., 2018. Benthic foraminifera distribution in a deltaic clinoform (São Francisco Delta, eastern Brazil): a reference study. J. Mar. Syst. 186, 1–16. https://doi.org/10.1016/j.jmarsys.2018.05.004.
De Santis, V., Caldara, M., 2016. Evolution of an incised valley system in the southern Adriatic Sea (Apulian margin): an onshore–offshore correlation. Geol. J. 51, 263–284. https://doi.org/10.1002/gj.2628.
De Santis, V., Caldara, M., de Torres, T., Ortiz, J.E., 2010. Stratigraphic units of the Apulian Tavoliere plain (Southern Italy): Chronology, correlation with marine isotope stages and implications regarding vertical movements. Sediment. Geol. 228 (3–4), 255–270. https://doi.org/10.1016/j.sedgeo.2010.05.001.
De Santis, V., Caldara, M., de Torres, T., Ortiz, J.E., 2014. Two middle Pleistocene warm stages in the terrace deposits of the Apulia region (southern Italy). Quat. Int. 332, 2–18. https://doi.org/10.1016/j.quaint.2013.10.009.
De Santis, V., Caldara, M., Pennetta, L., 2020a. Continuous backstepping of Holocene coastal barrier systems into incised valleys: insights from the Ofanto and Carapelle-Cervaro valleys. Water 12, 1799.
De Santis, V., Caldara, M., Pennetta, L., 2020b. Transgressive architecture of coastal barrier systems in the Ofanto incised valley and its surrounding shelf in response to stepped sea-level rise. Geosciences 10 (12), 497. https://doi.org/10.3390/geosciences10120497.
Dessandier, P.-A., Bonnin, J., Kim, J.-H., Bichon, S., Deflandre, B., Grémare, A., Sinninghe Damsté, J.S., 2016. Impact of organic matter source and quality on living benthic foraminiferal distribution on a river-dominated continental margin: a study of the Portuguese margin. Eur. J. Vasc. Endovasc. Surg. 121, 1689–1714. https://doi.org/10.1002/2015JG003231.
Di Bella, L., Casieri, S., 2011. Paleoenvironmental reconstruction of late Quaternary succession by foraminiferal assemblages of three cores from the San Benedetto del Tronto coast (Central Adriatic Sea, Italy). Quat. Int. 241, 169–183.
Di Bella, L., Frezza, V., Bergamin, L., Carboni, M.G., Falese, F., Martorelli, E., Tarragoni, C., Chiocci, F.L., 2014. Foraminiferal record and high-resolution seismic stratigraphy of the late Holocene succession of the submerged Ombrone River delta (Northern Tyrrhenian Sea, Italy). Quat. Int. 328-329, 287–300.
Di Bella, L., Pierdomenico, M., Bove, C., Casalbore, D., Ridente, D., 2021. Benthic foraminiferal response to sedimentary processes in a prodeltaic environment: the Gulf of Patti case study (Southeastern Tyrrhenian Sea). Geosciences 11, 220. https://doi.org/10.3390/geosciences11050220.
Díaz, J., Palanques, A., Nelson, C.H., Guillén, J., 1996. Morpho-structure and sedimentology of the Holocene Ebro prodelta mud belt (northwestern Mediterranean Sea). Cont. Shelf Res. 16, 435–456. https://doi.org/10.1016/0278-4343(95)00019-4.
Doglioni, C., 1993. Some remarks on the origin of foredeeps. Tectonophysics 228, 1–20. https://doi.org/10.1016/0040-1951(93)90211-2.
Doglioni, C., Mongelli, F., Pieri, P., 1994. The Puglia uplift (SE Italy): an anomaly in the foreland of the Apenninic subduction due to buckling of a thick continental lithosphere. Tectonics 13, 1309–1321. https://doi.org/10.1029/94TC01501.
Donnici, S., Serandrei Barbero, R., 2002. The benthic foraminiferal communities of the northern Adriatic continental shelf. Mar. Micropaleontol. 44, 93–123.
Fanget, A.-S., Bassetti, M.-A., Fontanier, C., Tudryn, A., Berné, S., 2016. Sedimentary archives of climate and sea-level changes during the Holocene in the Rhône prodelta (NW Mediterranean Sea). Clim. Past 12, 2161–2179. https://doi.org/10.5194/cp-12-2161-2016.
Ferraro, L., Alberico, I., Lirer, F., Vallefuoco, M., 2012. Distribution of benthic foraminifera from the southern Tyrrhenian continental shelf (South Italy). Rend. Fis. Acc. Lincei 23, 103–119. https://doi.org/10.1007/s12210-011-0160-2.
Fletcher, W.J., Zielhofer, C., 2013. Fragility of western Mediterranean landscapes during Holocene Rapid climate changes. Catena 103, 16–29.
Fontanier, C., Jorissen, F.J., Licari, L., Alexandre, A., Anschutz, P., Carbonel, P., 2002. Live benthic foraminiferal faunas from the Bay of Biscay: faunal density, composition, and microhabitats. Deep-Sea Res. I Oceanogr. Res. Pap. 49, 751–785. https://doi.org/10.1016/S0967-0637(01)00078-4.
Franzini, M., Leoni, L., Saitta, M., 1972. A simple method to evaluate the matrix effects in X-Ray fluorescence analysis. X-Ray Spectrom. 1, 151–154.
Frezza, V., Carboni, M.G., 2009. Distribution of recent foraminiferal assemblages near the Ombrone River mouth (Northern Tyrrhenian Sea, Italy). Rev. Micropaleontol. 52, 43–66. https://doi.org/10.1016/j.revmic.2007.08.007.
Frezza, V., Di Bella, L., 2015. Distribution of recent ostracods near the Ombrone River mouth (Northern Tyrrhenian Sea, Italy). Micropaleontology 61, 101–114.
Frezza, V., Carboni, M.G., Di Bella, L., 2012. Late Holocene paleoenvironmental evidences from foraminiferal assemblages in the Northern Tyrrhenian Sea (Southern Tuscany, Italy). Rend. Online Soc. Geol. It. 21, 1083–1085.

Garzanti, E., Andò, S., Vezzoli, G., 2009. Grain-size dependence of sediment composition and environmental bias in provenance studies. Earth Planet. Sci. Lett. 277, 422–432. https://doi.org/10.1016/j.epsl.2008.11.007.

Glaser, R., Riemann, D., Schönbein, J., Barriendos, M., Brázdil, R., Bertolin, C., Camuffo, D., Deutsch, M., Dobrovolný, P., van Engelen, A., Enzi, S., Halícková, M., Koenig, S.J., Kotyza, O., Limanówka, D., Macková, J., Sghedoni, M., Martin, B., Himmelsbach, I., 2010. The variability of European floods since AD 1500. Clim. Chang. 101, 235–256. https://doi.org/10.1007/s10584-010-9816-7.

Gliozzi, E., Grossi, F., 2008. Late Messinian lago-mare ostracod palaeoecology: a correspondence analysis approach. Palaeogeogr. Palaeoclimatol. Palaeoecol. 264, 288–295.

Goineau, A., Fontanier, C., Mojtahid, M., Fanget, A.-S., Bassetti, M.-A., Berné, S., Jorissen, F., 2015. Live–dead comparison of benthic foraminiferal faunas from the Rhône prodelta (Gulf of Lions, NW Mediterranean): development of a proxy for palaeoenvironmental reconstructions. Mar. Micropaleontol. 119, 17–33. https://doi.org/10.1016/j.marmicro.2015.07.002.

Gooday, A.J., Jorissen, F., Levin, L.A., Middelburg, J.J., Naqvi, S.W.A., Rabalais, N.N., Scranton, M., Zhang, J., 2009. Historical records of coastal eutrophication-induced hypoxia. Biogeosciences 6, 1707–1745. https://doi.org/10.5194/bg-6-1707-2009.

Goudeau, M.L.S., Grauel, A.L., Bernasconi, S.M., de Lange, G.J., 2013. Provenance of surface sediments along the southeastern Adriatic coast off Italy: an overview. Estuar. Coast. Shelf Sci. 134, 45–56. https://doi.org/10.1016/j.ecss.2013.09.009.

Greggio, N., Giambastiani, B.M.S., Campo, B., Dinelli, E., Amorosi, A., 2018. Sediment composition, provenance, and Holocene paleoenvironmental evolution of the Southern Po River coastal plain (Italy). Geol. J. 53, 914–928.

Griveaud, C., Jorissen, F., Anschutz, P., 2010. Spatial variability of live benthic foraminiferal faunas on the Portuguese margin. Micropaleontology 56 (3/4), 297–322.

Hammer, Ø., Harper, D.A.T., Ryan, P.D., 2001. PAST: paleontological statistics software package for education and data analysis. Palaeontol. Electron. 4, 1–9.

Hanebuth, T.J.J., Kinga, M.L., Lobo, F.J., Mendes, I., 2021. Formation history and material budget of Holocene shelf mud depocenters in the Gulf of Cadiz. Sediment. Geol. 421, 105956.

Heaton, T.J., Köhler, P., Butzin, M., Bard, E., Reimer, R.W., Austin, W.E.N., Bronk Ramsey, C., Grootes, P.M., Hughen, K.A., Kromer, B., 2020. Marine20—the marine radiocarbon age calibration curve (0–55,000 cal BP). Radiocarbon 62, 779–820. https://doi.org/10.1017/RDC.2020.68.

Jorissen, F.J., 1987. The distribution of benthic foraminifera in the Adriatic Sea. Mar. Micropaleontol. 12, 21–48. https://doi.org/10.1016/0377-8398(87)90012-0.

Jorissen, F.J., 1988. Benthic Foraminifera from the Adriatic Sea; Principles of Phenotypic Variation. Utrecht Micropaleontol, Bull, p. 37.

Jorissen, F., Nardelli, M.P., Almogi-Labin, A., Barras, C., Bergamin, L., Bicchi, E., El Kateb, A., Ferraro, L., McGann, M., Morigi, C., Romano, E., Sabbatini, A., Schweizer, M., Spezzaferri, S., 2018. Developing Foram-AMBI for biomonitoring in the Mediterranean: species assignments to ecological categories. Mar. Micropaleontol. 140, 33–45. https://doi.org/10.1016/j.marmicro.2017.12.006.

Kennedy, M.J., Pevear, D., Hill, R., 2002. Mineral surface control of organic carbon in black shale. Science 295, 657–660.

Laut, L.L.M., Clemente, I.M.M.M., Belart, P., Martins, M.V.A., Frontalini, F., Laut, V.M., Gomes, A., Boski, T., Lorini, M.L., Fortes, R.R., Rodrigues, M.A.C., 2016. Multiproxies (benthic foraminifera, ostracods and biopolymers) approach applied to identify the environmental partitioning of the Guadiana River Estuary (Iberian Peninsula). J. Sediment. Environ. 1 (2), 184–201.

Legendre, P., De Cáceres, M., 2013. Beta diversity as the variance of community data: dissimilarity coefficients and partitioning. Ecol. Lett. 16, 951–963.

Legendre, P., Gallagher, E.D., 2001. Ecologically meaningful transformations for ordination of species data. Oecologia 129, 271–280. https://doi.org/10.1007/s004420100716.

Leoni, L., Saitta, M., 1976. X-ray fluorescence analysis of 29 trace elements in rock and mineral standards. Rend. Soc. It. Miner. Pet. 32, 497–510.

Leoni, L., Menichini, M., Saitta, M., 1982. Determination of S, Cl and F in silicate rocks by X-Ray fluorescence analyses. X-Ray Spectrom. 11, 156–158.

Liaghati, T., Preda, M., Cox, M., 2003. Heavy metal distribution and controlling factors within coastal plain sediments, Bells Creek catchment, Southeast Queensland, Australia. Environ. Int. 29, 935–948.

Liquete, C., Lucchi, R.G., Garcia-Orellana, J., Canals, M., Masqué, P., Pasqual, C., Lavoie, C., 2010. Modern sedimentation patterns and human impacts on the Barcelona continental shelf (NE Spain). Geol. Acta 8, 169–187. https://doi.org/10.1344/105.000001528.

Lowe, J.J., Blockley, S., Trincardi, F., Asioli, A., Cattaneo, A., Matthews, I.P., Pollard, M., Wulf, S., 2007. Age modelling of late Quaternary marine sequences in the Adriatic: towards improved precision and accuracy using volcanic event stratigraphy. Cont. Shelf Res. 27, 560–582.

Luterbacher, J., García-Herrera, R., Akcer-On, S., Allan, R., Alvarez-Castro, M.-C., Benito, G., Booth, J., Büntgen, U., Cagatay, N., Colombaroli, D., Davis, B., Esper, J., Felis, T., Fleitmann, D., Frank, D., Gallego, D., Garcia-Bustamante, E., Glaser, R., Gonzalez-Rouco, F.J., Goosse, H., Kiefer, T., Macklin, M.G., Manning, S.W., Montagna, P., Newman, L., Power, M.J., Rath, V., Ribera, P., Riemann, D., Roberts, N., Sicre, M.A., Silenzi, S., Tinner, W., Tzedakis, P.C., Valero-Garcés, B., van der Schrier, G., Vannière, B., Vogt, S., Wanner, H., Werner, J.P., Willett, G., Williams, M.H., Xoplaki, E., Zerefos, C.S., Zorita, E., 2012. A review of 2000 years of Paleoclimatic evidence in the Mediterranean. In: Lionello, P. (Ed.), The Climate of the Mediterranean Region. Elsevier, pp. 87–185. https://doi.org/10.1016/B978-0-12-416042-2.00002-1.

Marchesini, M., Marvelli, S., 2017. Paesaggio vegetale e agricoltura nella Pianura padana in età romana. In: Lo Cascio, E., Maiuro, M. (Eds.), Popolazione e risorse nell'Italia del nord dalla romanizzazione ai Longobardi. Pragmateiai 28, Bari, pp. 289–304.

Maselli, V., Trincardi, F., 2013. Large-scale single incised valley from a small catchment basin on the western Adriatic margin (Central Mediterranean Sea). Glob. Planet. Chang. 100, 245–262.

Maselli, V., Trincardi, F., Asioli, A., Ceregato, A., Rizzetto, F., Taviani, M., 2014. Delta growth and river valleys: the influence of climate and sea level changes on the south Adriatic shelf (Mediterranean Sea). Quat. Sci. Rev. 99, 146–163.

Mendes, I., Dias, J.A., Schönfeld, J., Ferreira, Ó., Rosa, F., Gonzalez, R., Lobo, F.J., 2012. Natural and human-induced Holocene paleoenvironmental changes on the Guadiana shelf (northern Gulf of Cadiz). Holocene 22 (9), 1011–1024. https://doi.org/10.1177/0959683612437867.

Mendes, I., Lobo, F.J., Hanebuth, T.J.J., López-Quirós, A., Schönfeld, J., Lebreiro, S., Reguera, M.I., Antón, L., Ferreira, O., 2020. Temporal variability of flooding events of Guadiana River (Iberian Peninsula) during the middle to late Holocene: Imprints in the shallow-marine sediment record. Palaeogeogr. Palaeoclimatol. Palaeoecol. 556, 109900 https://doi.org/10.1016/j.palaeo.2020.109900.

Mercuri, A.M., Allevato, E., Arobba, D., Bandini Mazzanti, M., Bosi, G., Caramiello, R., Castiglioni, E., Carra, M.L., Celant, A., Costantini, L., Di Pasquale, G., Fiorentino, G., Florenzano, A., Guido, M., Marchesini, M., Mariotti Lippi, M., Marvelli, S., Miola, A., Montanari, C., Nisbet, R., Peña-Chocarro, L., Perego, R., Ravazzi, C., Rottoli, M., Sadori, L., Ucchesu, M., Rinaldi, R., 2015. Pollen and macroremains from Holocene archaeological sites: a dataset for the understanding of the bio-cultural diversity of the Italian landscape. Rev. Palaeobot. Palynol. 218, 250–266.

Mojtahid, M., Jorissen, F., Lansard, B., Fontanier, C., Bombled, B., Rabouille, C., 2009. Spatial distribution of live benthic foraminifera in the Rhône prodelta: faunal response to a continental–marine organic matter gradient. Mar. Micropaleontol. 70, 177–200. https://doi.org/10.1016/j.marmicro.2008.12.006.

Montenegro, M.E., Pugliese, N., 1996. Autecological remarks on the ostracod distribution in the Marano and Grado lagoons (northern Adriatic Sea, Italy). Boll. Soc. Paleontol. Ital. 3, 123–132.

Morigi, C., Jorissen, F.J., Fraticelli, S., Horton, B.P., Principi, M., Sabbatici, A., Capotondi, L., Curzi, P.V., Negri, A., 2005. Benthic foraminiferal evidence for the formation of the Holocene mud-belt and bathymetrical evolution in the Central Adriatic Sea. Mar. Micropaleontol. 57, 25–49.

Norbäck Ivarsson, L., Andrén, T., Moros, M., Andersen, T.J., Lönn, M., Andrén, E., 2019. Baltic Sea coastal eutrophication in a thousand year perspective. Front. Environ. Sci. 7, 88. https://doi.org/10.3389/fenvs.2019.00088.

Oldfield, F., Asioli, A., Accorsi, C.A., Mercuri, A.M., Juggins, S., Langone, L., Rolph, T., Trincardi, F., Wolff, G., Gibbs, Z., Vigliotti, L., Frignani, M., van der Post, K., Branch, N., 2003. A high resolution late Holocene palaeo-environmental record from the Central Adriatic Sea. Quat. Sci. Rev. 22, 319–342.

Owen, R.B., Lee, R., 2004. Human impacts on organic matter sedimentation in a proximal shelf setting, Hong Kong. Cont. Shelf Res. 24 (4–5), 583–602. https://doi.org/10.1016/j.csr.2003.11.004.

Pascual, A., Rodriguez-Lazaro, J., Martín-Rubio, M., Jouanneau, J.-M., Weber, O., 2008. A survey of the benthic microfauna (foraminifera, Ostracoda) on the Basque shelf, southern Bay of Biscay. J. Mar. Syst. 72, 35–63.

Pellegrini, C., Maselli, V., Cattaneo, A., Piva, A., Ceregato, A., Trincardi, F., 2015. Anatomy of a compound delta from the post-glacial transgressive record in the Adriatic Sea. Mar. Geol. 362, 43–59. https://doi.org/10.1016/j.margeo.2015.01.010.

Pellegrini, C., Tesi, T., Schieber, J., Bohacs, K.M., Rovere, M., Asioli, A., Nogarotto, A., Trincardi, F., 2021. Fate of terrigenous organic carbon in muddy clinothems on continental shelves revealed by stratal geometries: insight from the Adriatic sedimentary archive. Glob. Planet. Chang. 203, 103539 https://doi.org/10.1016/j.gloplacha.2021.103539.

Pellegrini, C., Sammartino, I., Schieber, J., Tesi, T., Paladini De Mendoza, F., Rossi, V., Chiggiato, J., Schroeder, K., Gallerani, A., Langone, L., Trincardi, F., Amorosi, A., 2023. On depositional processes governing along-strike facies variations of fine-grained deposits: Unlocking the Little Ice Age subaqueous clinothems on the Adriatic shelf. Sedimentology. https://doi.org/10.1111/sed.13162.

Piva, A., Asioli, A., Trincardi, F., Schneider, R.R., Vigliotti, L., 2008. Late-Holocene climate variability in the Adriatic Sea (Central Mediterranean). Holocene 18 (1), 153–167. https://doi.org/10.1177/0959683607085606.

Ravaioli, M., Alvisi, F., Vitturi, L.M., 2003. Dolomite as a tracer for sediment transport and deposition on the northwestern Adriatic continental shelf (Adriatic Sea, Italy). Cont. Shelf Res. 23, 1359–1377. https://doi.org/10.1016/S0278-4343(03)00121-3.

Rossi, V., Azzarone, M., Capraro, L., Faranda, C., Ferretti, P., Macrì, P., Scarponi, D., 2018. Dynamics of benthic marine communities across the Early-Middle Pleistocene boundary in the Mediterranean region (Valle di Manche, Southern Italy): biotic and stratigraphic implications. Palaeogeogr. Palaeoclimatol. Palaeoecol. 495, 127–138. https://doi.org/10.1016/j.palaeo.2017.12.042.

Rossi, V., Barbieri, G., Vaiani, S.C., Cacciari, M., Bruno, L., Campo, B., Marchesini, M., Marvelli, S., Amorosi, A., 2021. Millennial-scale shifts in microtidal ecosystems during the Holocene: dynamics anddrivers of change from the Po Plain coastal record (NE Italy). J. Quat. Sci. 36 (6), 961–979. https://doi.org/10.1002/jqs.3322.

Rovere, M., Pellegrini, C., Chiggiato, J., Campiani, E., Trincardi, F., 2019. Impact of dense bottom water on a continental shelf: an example from the SW Adriatic margin. Mar. Geol. 408, 123–143.

Scarponi, D., Nawrot, R., Azzarone, M., Pellegrini, C., Gamberi, F., Trincardi, F., Kowalewski, M., 2022. Resilient biotic response to long-term climate change in the Adriatic Sea. Glob. Chang. Biol. 28 (13), 4041–4053.

Schnedl, S.-M., Haselmair, A., Gallmetzer, I., Mautner, A.-K., Tomašových, A., Zuschin, M., 2018. Molluscan benthic communities at Brijuni Islands (northern

Adriatic Sea) shaped by Holocene Sea-level rise and recent human eutrophication and pollution. Holocene 28 (11), 1801–1817.
Sgarrella, F., Moncharmont Zei, M., 1993. Benthic Foraminifera of the Gulf of Naples (Italy): systematics and autoecology. Boll. Soc. Paleontol. Ital. 32, 145–264.
Sicre, M.-A., Jalali, B., Martrat, B., Schmidt, S., Bassetti, M.-A., Kallel, N., 2016. Sea surface temperature variability in the North Western Mediterranean Sea (Gulf of Lion) during the Common Era. Earth Planet. Sci. Lett. 456, 124–133. https://doi.org/10.1016/j.epsl.2016.09.032.
Sømme, T.O., Helland-Hansen, W., Martinsen, O.J., Thurmond, J.B., 2009. Relationships between morphological and sedimentological parameters in source-to-sink systems: a basis for predicting semi-quantitative characteristics in subsurface systems. Basin Res. 21, 361–387. https://doi.org/10.1111/j.1365-2117.2009.00397.x.
Spagnoli, F., Bartholini, G., Dinelli, E., Giordano, P., 2008. Geochemistry and particle size of surface sediments of Gulf of Manfredonia (Southern Adriatic Sea). Estuar. Coast. Shelf Sci. 80, 21–30. https://doi.org/10.1016/j.ecss.2008.07.008.
Spagnoli, F., Dell'Anno, A., De Marco, A., Dinelli, E., Fabiano, M., Gadaleta, M.V., Ianni, C., Loiacono, F., Manini, E., Marini, M., Mongelli, G., Rampazzo, G., Rivaro, P., Vezzulli, L., 2010. Biogeochemistry, grain size and mineralogy of the central and southern Adriatic Sea sediments: a review. Chem. Ecol. 26, 19–44.
Spagnoli, F., Dinelli, E., Giordano, P., Marcaccio, M., Zaffagnini, F., Frascari, F., 2014. Sedimentological, biogeochemical and mineralogical facies of Northern and Central Western Adriatic Sea. J. Mar. Syst. 139, 183–203. https://doi.org/10.1016/j.jmarsys.2014.05.021.
Spagnoli, F., De Marco, R., Dinelli, E., Frapiccini, E., Frontalini, F., Giordano, P., 2021. Sources and metal pollution of sediments from a coastal area of the central western Adriatic Sea (southern Marche region, Italy). Appl. Sci. 11, 1118.
Stalder, C., ElKateb, A., Spangenberg, J.E., Terhzaz, L., Vertino, A., Spezzaferri, S., 2021. Living benthic foraminifera from cold-water coral ecosystems in the eastern Alboran Sea, Western Mediterranean. Heliyon 7, e07880. https://doi.org/10.1016/j.heliyon.2021.e07880.
Szymczak-Żyła, M., Krajewska, M., Witak, M., Ciesielski, T.M., Ardelan, M.V., Jenssen, B. M., Goslar, T., Winogradow, A., Filipkowska, A., Lubecki, L., Zamojska, A., Kowalewska, G., 2019. Present and past-millennial eutrophication in the Gulf of Gdańsk (southern Baltic Sea). Paleoceanogr. Paleoclimatol. 34, 136–152. https://doi.org/10.1029/2018PA003474.
Tentori, D., Milli, S., Marsaglia, K.M., 2018. A source-to-sink compositional model of a present highstand: an example in the low-rank Tiber depositional sequence (Latium Tyrrhenian margin, Italy). J. Sediment. Res. 88, 1238–1259. https://doi.org/10.2110/jsr.2018.60.
Tesi, T., Miserocchi, S., Goni, M.E.A., Langone, L., Boldrin, A., Turchetto, M., 2007. Organic matter origin and distribution in suspended particulate materials and surficial sediments from the western Adriatic Sea (Italy). Estuar. Coast. Shelf Sci. 73 (3–4), 431–446.
Trincardi, F., Cattaneo, A., Asioli, A., Correggiari, A., Langone, L., 1996. Stratigraphy of the late-Quaternary deposits in the central Adriatic basin and the record of short-term climatic events. In: Oldfield, F., Guilizzoni, P. (Eds.), Palaeoenvironmental Analysis of Italian Crater Lake and Adriatic Sediments, Memorie dell'Istituto Italiano di Idrobiologia, vol. 55, pp. 39–70.
Trincardi, F., Campiani, E., Correggiari, A., Foglini, F., Maselli, V., Remia, A., 2014. Bathymetry of the Adriatic Sea: The legacy of the last eustatic cycle and the impact of modern sediment dispersal. J. Maps 10 (1), 151–158. https://doi.org/10.1080/17445647.2013.864844.
Tropeano, M., Sabato, L., Pieri, P., 2002. Filling and cannibalization of a foredeep: the Bradanic Trough, southern Italy. Geol. Soc. Spec. Publ. 191, 55–79.
Turchetto, M., Boldrin, A., Langone, L., Miserocchi, S., Tesi, T., Foglini, F., 2007. Particle transport in the Bari canyon (southern Adriatic Sea). Mar. Geol. 246 (2–4), 231–247.
Vacchi, M., Marriner, N., Morhange, C., Spada, G., Fontana, A., Rovere, A., 2016. Multiproxy assessment of Holocene relative sea-level changes in the western Mediterranean: sea-level variability and improvements in the definition of the isostatic signal. Earth Sci. Rev. 155, 172–197. https://doi.org/10.1016/j.earscirev.2016.02.002.
Vacchi, M., Joyse, K.M., Kopp, R.E., Marriner, N., Kaniewski, D., Rovere, A., 2021. Climate pacing of millennial sea-level change variability in the central and western Mediterranean. Nat. Commun. 12, 4013. https://doi.org/10.1038/s41467-021-24250-1.
Van Der Zwaan, G.J., Jorissen, F.J., 1991. Biofacial patterns in river-induced shelf anoxia. Geol. Soc. Lond. Spec. Publ. 58, 65–82. https://doi.org/10.1144/GSL.SP.1991.058.01.05.
Weltje, G.J., Brommer, M.B., 2011. Sediment-budget modelling of multi-sourced basin fills: application to recent deposits of the western Adriatic mud wedge (Italy). Basin Res. 23, 291–308. https://doi.org/10.1111/j.1365-2117.2010.00484.x.
Zecchin, M., Catuneanu, O., 2013. High-resolution sequence stratigraphy of clastic shelves I: units and bounding surfaces. Mar. Pet. Geol. 39, 1e25.
Zecchin, M., Gordini, E., Ramella, R., 2015. Recognition of a drowned delta in the northern Adriatic Sea, Italy: Stratigraphic characteristics and its significance in the frame of the early Holocene Sea-level rise. Holocene 25 (6), 1027–1038.